Mean-field thalamocortical modeling of longitudinal EEG acquired during intensive meditation training

Manish Saggar [a,b,*], Anthony P. Zanesco [c,d], Brandon G. King [c,d], David A. Bridwell [e], Katherine A. MacLean [f], Stephen R. Aichele [c,d], Tonya L. Jacobs [d], B. Alan Wallace [g], Clifford D. Saron [d,h], Risto Miikkulainen [b]

[a] Department of Psychiatry and Behavioral Sciences, Stanford University, Stanford, CA, USA
[b] Department of Computer Science, University of Texas at Austin, TX, USA
[c] Department of Psychology, University of California, Davis, CA, USA
[d] Center for Mind and Brain, University of California, Davis, CA, USA
[e] Mind Research Network, Albuquerque, NM, USA
[f] Department of Psychiatry and Behavioral Sciences, Johns Hopkins University, Baltimore, MD, USA
[g] Santa Barbara Institute for Consciousness Studies, Santa Barbara, CA, USA
[h] The M.I.N.D. Institute, University of California, Davis, Sacramento, CA, USA

ARTICLE INFO

ABSTRACT

Meditation training has been shown to enhance attention and improve emotion regulation. However, the brain processes associated with such training are poorly understood and a computational modeling framework is lacking. Modeling approaches that can realistically simulate neurophysiological data while conforming to basic anatomical and physiological constraints can provide a unique opportunity to generate concrete and testable hypotheses about the mechanisms supporting complex cognitive tasks such as meditation. Here we applied the mean-field computational modeling approach using the scalp-recorded electroencephalogram (EEG) collected at three assessment points from meditating participants during two separate 3-month-long shamatha meditation retreats. We modeled cortical, corticothalamic, and intrathalamic interactions to generate a simulation of EEG signals recorded across the scalp. We also present two novel extensions to the mean-field approach that allow for: (a) non-parametric analysis of changes in model parameter values across all channels and assessments; and (b) examination of variation in modeled thalamic reticular nucleus (TRN) connectivity over the retreat period. After successfully fitting whole-brain EEG data across three assessment points within each retreat, two model parameters were found to replicably change across both meditation retreats. First, after training, we observed an increased temporal delay between modeled cortical and thalamic cells. This increase provides a putative neural mechanism for a previously observed reduction in individual alpha frequency in these same participants. Second, we found decreased inhibitory connection strength between the TRN and secondary relay nuclei (SRN) of the modeled thalamus after training. This reduction in inhibitory strength was found to be associated with increased dynamical stability of the model. Altogether, this paper presents the first computational approach, taking core aspects of physiology and anatomy into account, to formally model brain processes associated with intensive meditation training. The observed changes in model parameters inform theoretical accounts of attention training through meditation, and may motivate future study on the use of meditation in a variety of clinical populations.

© 2015 Elsevier Inc. All rights reserved.

Introduction

In traditional Buddhist thought, meditation refers to a process of familiarization (Tibetan *gom*) with or cultivation (Sanskrit *bhavana*) of particular mental states and cognitive capacities through the repeated observation, investigation, and recollection of mental processes and events (Langri, 2009; Wallace, 2005). Meditation is thus conceptualized as a form of *mental training* in which the practitioner engages in mental exercises in order to develop beneficial psychological, cognitive, and motivational traits (Walsh and Shapiro, 2006; Lutz et al., 2008), and attempts to gain deeper insight into their mental life. This conceptualization of meditation as a developmental process shares considerable theoretical overlap with cognitive and neuroscientific theories of learning, development, and neuroplasticity (Slagter et al., 2011). Contemporary psychological accounts of meditation have therefore argued that it is possible to understand and characterize the neurocognitive framework associated with meditation in terms of established features of attention and cognitive control (e.g., Hölzel et al., 2011; Lutz et al., 2008).

* Corresponding author at: 401 Quarry Road, MC 5795, Department of Psychiatry and Behavioral Sciences, Stanford University, Stanford, CA, USA.
E-mail address: saggar@stanford.edu (M. Saggar).

Among the practices utilized within various Buddhist traditions are a class of attention-regulatory techniques designed to promote attentional stability and vividness, traditionally termed *shamatha* (lit. calm abiding; Wallace, 2005, 2006). During shamatha practice, practitioners voluntarily direct and maintain attention on an external or internal object or domain of focus (e.g., sensations of the breath), monitoring if attention is on the intended target, and gently reorienting attention whenever it strays or becomes lax. A number of studies have shown that training with shamatha and related focused-attention (FA) meditation techniques is associated with enhanced cognitive control and improved attention regulation. For example, studies of intensive training in such meditation techniques have demonstrated improvements in attentional stability (Lutz et al., 2009; MacLean et al., 2010) and alerting (Jha et al., 2007), sustained response inhibition (Sahdra et al., 2011), efficiency in information processing (Slagter et al., 2007; van Vugt and Jha, 2011), and perceptual discrimination (MacLean et al., 2010). Moore and colleagues reported that regular but non-intensive practice of FA-style meditation over 16 weeks can lead to enhanced attentional processing and increased efficiency of resource allocation during object recognition processes (Moore et al., 2012). Overall, these studies have shown that regular practice of shamatha and related FA meditation may lead to improvements in behavioral measures of attention and cognitive control.

Despite the sizeable amount of attention-related research on meditation training, the brain processes associated with these behavioral improvements are not well characterized. One avenue for investigating the neural correlates of meditation has been to examine the patterns of brain activation that co-occur during the practice of specified meditation techniques. These studies have typically relied upon measuring cortical oscillatory activity (scalp-recorded EEG) and have more recently employed other neuroimaging modalities such as functional Magnetic Resonance Imaging (Cahn and Polich, 2006). Although a number of studies have suggested that experienced meditation practitioners show greater recruitment of attention-related brain networks during practice of FA meditation (Brefczynski-Lewis et al., 2007; Hasenkamp and Barsalou, 2012; Hasenkamp et al., 2012; Saggar et al., 2012), there is no consensus on the extent or specificity of neural activity associated with such practice. Investigation of the neural processes recruited during FA practice is complicated by the difficulty of experimentally controlling participants' unobservable mental states, which cannot be corroborated conclusively through external measurement. Thus, much of this research relies on inferences regarding the engagement of specific cognitive processes drawn solely from observed neural activity. Furthermore, relatively little is known about how intensive training alters state-specific neural activity. Characterizing how meditation state-specific neural activity may be affected through training (e.g., Saggar et al., 2012) will aid our understanding of how the repeated recruitment of large-scale brain networks during meditation practice may be related to the development of enduring psychological traits.

In our previous work (Saggar et al., 2012), we examined patterns of scalp-recorded oscillatory activity (EEG) while participants engaged in 6 min of mindfulness of breathing practice in which they focused on the tactile sensations of the breath. Training and wait-list control group participants each underwent a three-month intensive shamatha meditation retreat. Ongoing cortical oscillatory activity was assessed using spectral analysis of dense-array EEG at three assessment points (pre-, mid-, and post-retreat) across two separate training periods. Two robust changes in cortical activity were replicated across the training interventions: 1) significant reductions in beta-band power, bilaterally over anterior–central and posterior scalp regions, and 2) reductions in state-related global individual alpha frequency (IAF; Klimesch, 1999). Training-related changes in beta-band power were interpreted as indicating increased cortical activation of sensory- and attention-related brain networks recruited during voluntary focus on the tactile sensations of the breath. In the context of these changes in spectral power, reductions in IAF were interpreted as suggesting that participants' capacity to focus attention on the breath was less effortful following

training. These findings provide evidence of longitudinal changes in meditation state-related brain oscillatory activity during mindfulness of breathing that may potentially support long-term improvements in attention regulation.

In studies such as Saggar et al., 2012, the ability to draw clear conclusions about psychological processes from presumed meditation state-related brain activity is limited by a number of methodological and inferential constraints. During meditation practice, meditation practitioners typically engage in covert or internalized tasks for which there are no obvious external markers of performance or compliance. Although researchers often provide specific instructions to practitioners to engage in particular meditation techniques, there is no direct way to confirm that participants are following instructions similarly. Brain activity observed during meditation may also reflect cognitive states not directly related to implementing the techniques themselves (e.g., mind wandering). Inferences regarding the role of observed brain activity as reflecting state-specific cognitive processes must rely on references to patterns of activity identified in other task domains. Potential avenues for resolving these ambiguities include pairing induced state-related brain activity with practitioners' first-person introspective reports (i.e., neurophenomenology; Desbordes and Negi, 2013; Lutz and Thompson, 2003), and correlational approaches that relate measures of meditation state-related brain activity to behavioral performance on tasks presumed to share cognitive mechanisms with specified techniques. Another approach involves utilizing computational models of state-related activity to better characterize presumed mechanisms of neural activation from the recorded EEG itself. Such models can be used to generate targeted hypotheses regarding the cortico-cortical and subcortico-cortical dynamics associated with practice and training (Kerr et al., 2013). Here, we utilize the later approach of computational modeling to formally characterize longitudinal changes in cortical activity associated with intensive focused-attention meditation training (Saggar et al., 2012). Computational models provide a mathematical approach that allows for simulating complex phenomena for which closed-form analytical solutions do not exist and for generating concrete novel hypotheses for future research.

Effective computational models are based on realistic biophysical and anatomical constraints involving conceptual understanding of the processes involved. The cognitive model of attention proposed by Posner and Peterson (1990) articulates a number of attentional component processes that are relevant to conceptions of shamatha and related FA meditation practice, such as attentional alerting, orienting, and monitoring. Neuroimaging studies investigating this cognitive model (Corbetta and Shulman, 2002; Fan et al., 2005) have highlighted the role of fronto-parietal cortical networks and thalamic sub-cortical areas in attention regulation (Kastner et al., 2012) and cognitive control (Dosenbach et al., 2008). Additionally, these findings have been corroborated by neuroimaging studies of large-scale cognitive-control networks (Bressler and Menon, 2010; Menon, 2011). Based on these studies, we propose to model the neurophysiological mechanisms associated with cognitive processes engaged during FA meditation by incorporating cortical and thalamic components involved in attention regulation and by investigating the utility of a biophysical model of corticothalamocortical loops to account for observed longitudinal changes in scalp-recorded EEG.

There are a wide range of approaches available for the computational modeling of EEG data, including purely phenomenological approaches (Isaksson et al., 1981; Wright et al., 1990), mean-field modeling (i.e., Freeman, 1972, 1987; Jirsa et al., 2010; Lopes da Silva et al., 1974; Nunez, 1974a,b; Robinson et al., 2001b; Wilson and Cowan, 1972, 1973), and detailed neural networks (Lagerlund and Sharbrough, 1989; Lumer et al., 1997; Reimann et al., 2013; Traub et al., 1997; Wilson and Bower, 1992). Whereas phenomenological approaches simulate data without incorporating anatomical information, mean-field modeling allows for simulation at the level of neural populations while incorporating some anatomical information. Discounting

volume conduction, each EEG sensor (~5 mm in diameter) represents the aggregate synaptic activity of a population of hundreds of thousands of neurons (Pizzagalli, 2007). The complexities of population dynamics, resulting from the complexity of cortical micro-circuitry, creates a challenge for detailed modeling. However, an approximation of mean population activity may be modeled for each sensor using mean-field modeling, while keeping intact desired assumptions regarding overall corticothalamic anatomical and physiological constraints.

We used the Robinson et al. (2001b) Mean-Field Model (henceforth referred to as R-MFM), in which EEG spectra at the scalp are simulated using postulated corticocortical, corticothalamic, and intrathalamic loops. The R-MFM was chosen because scalp-recorded EEG data are generated primarily by the summation of excitatory and inhibitory post-synaptic potentials in the pyramidal cells of the cortex (Pizzagalli, 2007; Speckmann and Altrup, 1993), and because oscillations in subcortical areas, especially the thalamus, and oscillations due to corticothalamocortical interactions are considered to be major contributors to the generation of cortical alpha and beta rhythms (Robinson et al., 2002; Steriade, 2005; Steriade et al., 1993). In humans, studies combining EEG measures with positron emission tomography and fMRI have provided direct evidence for a relation between glucose metabolic activity in the thalamus and scalp-recorded EEG alpha power (Goldman et al., 2002; Larson et al., 1998; Schreckenberger et al., 2004). In a recent review, using a neural network model of a single cortical column in the primary somatosensory cortex (SI) (Jones et al., 2007; Jones, 2009), Kerr et al. (2013) hypothesized that interactions between thalamic regions and SI may facilitate attentional modulation of alpha rhythms (7–14 Hz) during FA meditation practice. Further, research on long-term meditators has also invoked the role of thalamic nuclei (esp. the reticular nucleus) in regulating and sustaining attention on the object of meditative focus (Austin, 2013; Guglietti et al., 2012; Newberg and Iversen, 2003). Thus, by modeling interactions between corticocortical, corticothalamic and intrathalamic cells in meditation-state related EEG data, our computational approach can provide a framework for generating targeted hypotheses, which can motivate empirical verification using multimodal non-invasive approaches in future research.

In the present investigation, we first used R-MFM to simulate whole-brain EEG data obtained while participants engaged in 6 min of breath-focused FA meditation practice. Next, using standard model-fitting procedures, the R-MFM parameters were refined for each participant in order to fit the simulated data to the observed EEG spectra collected at three assessment points over the 3-month training period. Finally, using inverse computational modeling, we explored longitudinal changes in model parameters to examine the effects of intensive meditation training on changes in corticocortical, corticothalamic, and intrathalamic parameters.

We also present two novel extensions to the R-MFM. First, using nonparametric statistical testing, we analyze longitudinal changes in model parameters across the whole-brain, rather than for single channels, as was done in previous applications of R-MFM; (Robinson et al., 2003a). This approach allows for analysis of changes in whole-brain EEG topography associated with intensive meditation training. Second, we explore how simulated connectivity patterns in the TRN may change over time. This extended model will henceforth be referred to as ER-MFM. Although these proposed extensions were developed to analyze meditation data, they can be applied to model longitudinal changes in corticothalamic architecture and dynamics within any EEG or MEG dataset.

Methods

Study design

Two three-month long residential meditation retreats were held at a scenic meditation center (Shambhala Mountain Center) in Red Feather Lakes, CO. Participants lived and practiced meditation onsite for the duration of training. Two separate groups of 30 participants were tested during the initial 3-month retreat: an in-residence retreat group undergoing training (RG1) and a matched wait-list control group (CG) that was flown to the retreat center for each assessment. The CG did not receive training during this period, but was tested using procedures identical to RG1. In the second retreat, the same CG participants underwent training that was formally identical to the training of RG1 participants during the initial retreat. Thus, we analyzed three datasets from two groups of participants: RG1 and CG during the initial retreat, and CG as training participants during the second retreat (subsequently referred to as RG2). The institutional review board of the University of California, Davis, approved all study procedures.

Participants

Data from 22 individuals in each participant group (initial retreat and wait-list control) were included in all analyses. Data for the remaining participants were removed due to poor signal quality and technical issues (see Saggar et al, 2012). Initial retreat and wait-list control participants included in the final sample did not differ (all $ps > .05$) in age (RG1: $M = 49.5$ years, $SD = 13.5$, CG: $M = 44.2$ years, $SD = 15.8$), gender (RG1: 12 female, CG: 11 female), or estimated lifetime meditation experience (RG1: $M = 2855.6$ h, $SD = 2994.1$, CG: $M = 2272.7$ h, $SD = 2326.3$).

Training

Dr. B. Alan Wallace, an established Buddhist teacher, contemplative, and scholar, served as the meditation instructor during both retreats. Meditation training was comprised of two general classes of techniques from the Buddhist contemplative tradition: shamatha techniques involving directing and sustaining attention on a chosen object and ancillary techniques involving the generation of benevolent aspirations for the well-being of oneself and others (Sahdra et al., 2011; Wallace, 2006). Shamatha techniques included *mindfulness of breathing*, in which attention is directed toward the breath; *observing mental events*, in which attention is directed toward the whole field of mental experience (e.g., thoughts, images, sensations); and *observing the nature of consciousness*, in which attention rests in the clear and cognizant experience of being aware. These shamatha practices are defined as such because they each aim to cultivate stable, clear, and effortless, single-pointed concentration (Wallace, 2006). Although these practices incorporate features commonly ascribed to focused-attention techniques, they may additionally share features of other classes of techniques, such as open-monitoring (OM; Lutz et al., 2008). Beneficial aspirations included practices that aim to cultivate *loving-kindness*, *compassion*, *empathic joy*, and *equanimity* (Wallace, 2006). Participants in RG1 (N = 22) spent an average of 5.7 h per day ($SD = 1.5$) practicing shamatha techniques (mindfulness of breathing $M = 2.10$ h, $SD = 2.16$; observing mental events $M = 1.74$ h, $SD = 2.22$; and observing nature of consciousness $M = 1.86$ h, $SD = 2.11$), and participants in RG2 (N = 22) spent an average of 5.4 h per day ($SD = 1.5$) on shamatha techniques (mindfulness of breathing $M = 3.16$ h, $SD = 1.84$; observing mental events $M = 1.00$ h, $SD = 1.23$; and observing nature of consciousness $M = 1.19$ h, $SD = 1.12$). The retreat groups (RG1, RG2) did not differ on the amount of time spent practicing solitary shamatha meditation ($t(42) = 0.49$, $p = .63$). Participants met twice daily for group meditation practice and discussion guided by Dr. Wallace. Participants also met one-on-one with Dr. Wallace on a weekly basis for advice, clarification, and guidance.

EEG data collection and preprocessing

Dense-array scalp EEG was recorded from 88 locations (equidistant montage, www.easycap.de) using a Biosemi Active2 system (www.biosemi.com) with 24-bit resolution sampled at 2048 Hz while participants engaged in a 12-min period of silent, eyes-closed *mindfulness of breathing* FA meditation. Participants were assessed at the beginning (T1), middle (T2), and end (T3) of each three-month retreat. During each assessment, the meditation began with approximately 50 s of audio instructions (provided below), recorded by Dr. Wallace:

"During the next 12 minutes, engage in the practice of mindfulness of breathing, focusing your attention on the tactile sensations at the apertures of your nostrils or just above your upper lip. With each inhalation arouse your attention and focus clearly on these tactile sensations. With each out-breath continue to maintain your attention upon the tactile sensations, while relaxing your body and mind, releasing any involuntary thoughts that may arise. So in this way maintain an ongoing flow of mindfulness, arousing with each in-breath, relaxing with each out-breath."

A recorded sound ("chime") signaled the end of the 12-minute meditation period. Continuous EEG was recorded over this entire period. However, due to an error in data acquisition at T1, only the first 6 min of data was recorded for some subjects. To allow for comparisons across all time points and datasets, we restricted analyses to the first 6 min of meditation across all three assessments in both retreats.

The 88-channel EEG data were band-pass filtered offline between 0.1 and 200 Hz. Second-order blind source identification (Belouchrani et al., 1993) was used to derive and separate non-neural signal contaminants from the ongoing electrical brain activity. Sources of putative non-neural origin were identified using a novel *s*emi-auto*m*atic *ar*tifact *r*emoval *too*l (SMART, available at http://stanford.edu/~saggar/Software.html). Extensive details regarding artifact identification and removal procedures can be found in Saggar et al. (2012). Special attention was given to remove sources due to muscular artifacts (aka electromyogram or EMG). Such sources were identified using low auto correlation values, broadband power across all frequencies and localized topographical locations (Saggar et al., 2012). After artifact removal, the 88-channel EEG data were reconstructed and transformed into a standard 81-channel montage (international 10–10 system), using spherical spline interpolation (Perrin et al., 1989). Interpolations were accomplished using Brain Electrical Source Analysis software (BESA 5.2; www.besa.de) with a smoothing parameter value (λ) of 2×10^{-6}. This transformation ensured that channel locations were standardized and that the number of channels remained consistent across participants. Eight channels (AF9, Fp1, Fpz, Fp2, Nz, AF10, CB1, CB2) from the 81-channel montage were excluded because information from the nearest corresponding electrode sites was not fully available in the original montage, yielding a final 73-channel montage for the reconstructed EEG. These reconstructed data were then transformed to a reference-free estimation of scalp current density (CSD; Kayser and Tenke, 2006).

Experimental EEG measures: power spectrum and individual alpha frequency estimation

The 6 min of reconstructed, artifact-free continuous EEG data were divided into two-second segments with 75% overlap. Power spectra were then calculated for each of these segments using the multi-tapered power spectral density estimation method (Mitra and Pesaran, 1999; Oostenveld et al., 2011) using in-house scripts implemented in MATLAB (MATLAB, 2010). Multi-tapered estimation improves power spectra estimation by obtaining multiple estimates from each sample.

Individual alpha frequency (IAF) was estimated using the center of gravity method for the frequency range of 7 Hz (f_1) to 14 Hz (f_2) (Klimesch, 1999),

$$\alpha_{IAF} = \frac{\sum_{i=f_1}^{f_2} (a(f_i) \times f_i)}{\sum_{i=f_1}^{f_2} (a(f_i))}, \tag{1}$$

where power-spectral estimates at frequency f_i are denoted by $a(f_i)$. The α_{IAF} values were calculated for each channel and were averaged across all channels to obtain a single IAF value per participant.

Model architecture

The Robinson et al. (2001b) mean-field modeling approach employs corticothalamic architecture and dynamics to simulate scalp EEG, and is based on earlier works on continuum modeling of EEG (Freeman, 1975; Liley and Wright, 1994; Lopes da Silva et al., 1974; Nunez, 1974a; Rennie et al., 1999; Robinson et al., 1997, 1998; Wilson and Cowan, 1973). This approach incorporates basic neurophysiological principles and structures, including transmission delays in axonal propagation, excitatory and inhibitory neural populations, and length- or range-dependent connections between cortical and subcortical populations (an overview is presented in Fig. 1 and a description of physiological limits is listed in Table 1). The R-MFM has been successfully used to reproduce various temporal and spectral properties of EEG data, such as evoked potentials (Kerr et al., 2008, 2010), seizure dynamics (Breakspear et al., 2006; Robinson et al., 2002), scalp-recorded EEG power spectra (Rennie et al., 2002; Robinson et al., 2001b; Rowe et al., 2004a), inter-channel coherence and correlation (Robinson et al., 2003a), and changes due to aging in healthy adults (Kerr et al., 2010, 2011; van Albada et al., 2010).

Model simulation and data fitting

First, all 73 EEG channels were independently modeled using the R-MFM. This approach assumes spatial uniformity and local independence in model parameters (i.e., a change in a parameter value at a distant channel will not affect the spectrum of the channel under observation). Thus, while modeling each channel, the values of parameters are chosen such that the modeled spectrum for each channel matches the experimental EEG spectrum. This approach is known as the local effective value (LEV) model (O'Connor and Robinson, 2004) and, although a first approximation, is both analytically tractable and computationally light (O'Connor and Robinson, 2004). For eyes-closed states, it has been shown that the local independence assumption of the LEV model is maintained within constraints of the model, except for low frequencies (i.e., <2 Hz) and at alpha frequency. However, this non-independence at alpha frequency is much smaller in magnitude than analogous effects at lower frequencies (O'Connor and Robinson, 2004).

Although care was taken to remove artifactual sources of noise (especially electromyographic activity (EMG) due to scalp muscle tension) during preprocessing and post-SOBI reconstruction of EEG data, a parameter for remaining EMG artifact was included in the estimation of power spectrum for each channel, as follows,

$$P_{est}(f) = P_{EEG}(f) + P_{EMG}(f). \tag{2}$$

No additional smoothing was performed on the experimentally recorded spectrum. The χ^2 error between the estimated spectrum ($P_{est}(f)$) and the experimentally obtained spectrum ($P_{exp}(f)$) was reduced using the trust-region-reflective constrained optimization
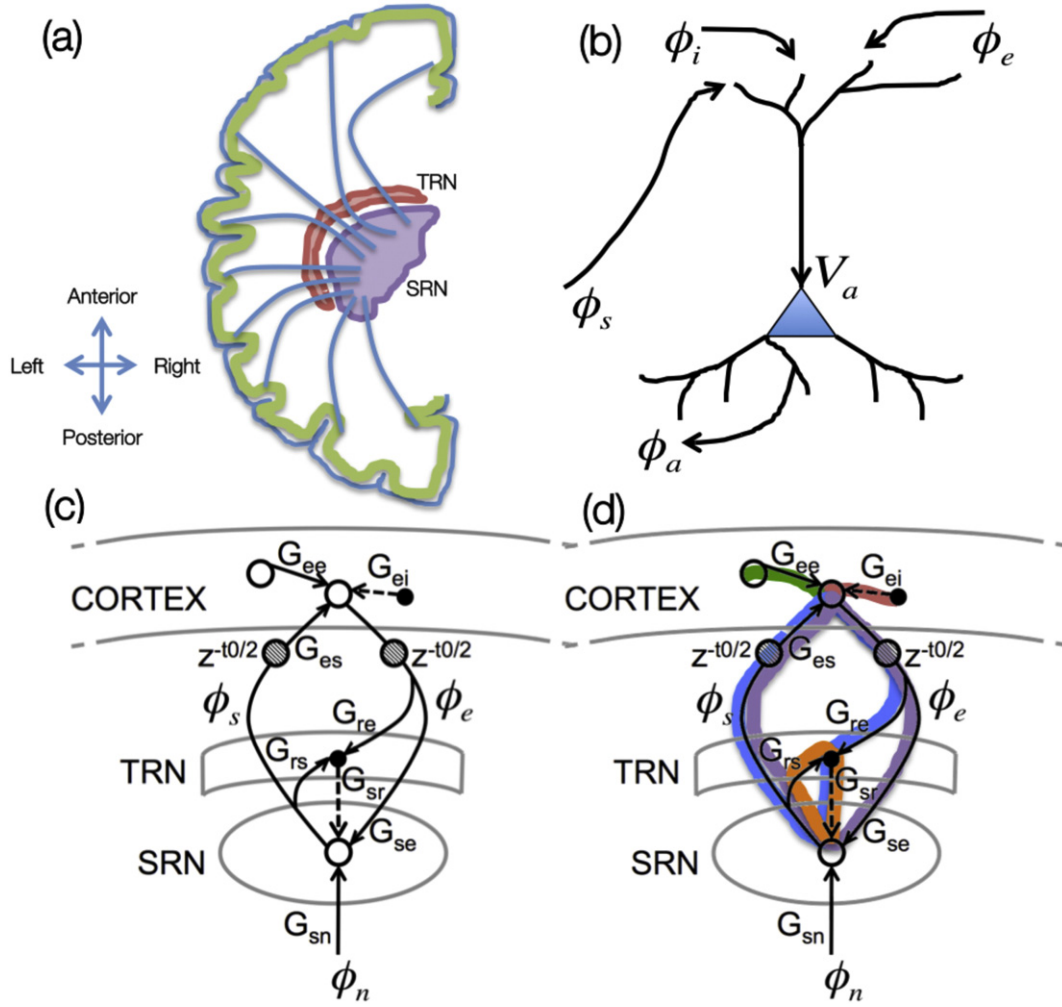
Fig. 1. The cortico-cortical, cortico-thalamo-cortical, and intrathalamic parameters of the R-MFM. (a) A schematic of cortico-thalamic connections in the left hemisphere, via the reticular nucleus of the thalamus (TRN). (b) Basic neuronal physiology incorporated in the model, shown in a cortical neuron. Synaptic connections at the dendritic tree are shown emanating from pulse-rate fields ϕ_b, where, b = e, i, s for cortical excitatory, inhibitory and subcortical connections, respectively. Somatic membrane potential is shown as V_a, where a = e, i with resultant impulse firing rate Q_a and the spread of action potentials as field ϕ_a, along the axons. (c) A schematic showing primary pathways between cortex, TRN, and thalamic secondary relay nuclei (SRN). Dashed lines represent inhibitory connections while solid lines represent excitatory ones. G_{ei} depicts the projections between local excitatory and inhibitory neurons in the cortex, while G_{ee} depicts similar projections between excitatory cortical neurons. These excitatory pyramidal neurons also project (through ϕ_e) to the thalamus, where signals may propagate (i) via TRN and then SRN with gain $G_{esre} = G_{es}G_{sr}G_{re}$, or (ii) directly via SRN with gain $G_{ese} = G_{es}G_{se}$. The SRN projects back (through ϕ_s) to the cortex, parametrized as the gain G_{es}. Within the thalamus, the intrathalamic loop has the gain $G_{srs} = G_{sr}G_{rs}$. Cortical activation (through sensory input) occurs via ϕ_n and ϕ_s with the gain $G_{es}G_{sn}$. The diagram is adapted from Rowe et al. (2005). (d) Model parameters that were inspected using longitudinal analysis. Five model parameters related to the strength or efficacy of the corresponding loops are shown in the figure: cortico-cortical excitatory (G_{ee}; in green), cortico-cortical inhibitory (G_{ei}; in red), cortico-thalamo-cortical via TRN (G_{esre}; in blue), cortico-thalamo-cortical without TRN (G_{ese}; in purple), and intrathalamic loop (G_{srs}; in orange). Five other parameters (not shown in the figure) were also inspected longitudinally: cortical damping rate (γ_e), dendritic decay rate (α), conduction delay in the signal from cortex to thalamus and back (t_0), normalization parameter for the spectrum (P_0), and normalization parameter for the EMG component (A).

algorithm (Coleman and Li, 1993), implemented in MATLAB, in which χ^2 is calculated for each site as

$$\chi^2 = \sum_{i=1}^{N} \left[\log\left(P_{exp}(f_i)\right) - \log(P_{est}(f_i)) \right]^2. \qquad (3)$$

The range for parameter values was bounded using the physiology-based limits presented in Table 1.

Model extension 1: longitudinal analysis

To model longitudinal changes in EEG data associated with meditation training, the R-MFM was extended to investigate changes in parameter values across assessment points (T1, T2, and T3) for all 73 channels separately for both retreats. In this extended approach (ER-MFM), spatiotemporal changes in model parameters were examined using nonparametric cluster-based permutation testing (Maris and Oostenveld, 2007) using FieldTrip (Oostenveld et al., 2011), an

open-source toolbox implemented in MATLAB. This approach has been used previously for analyzing changes in power spectra and coherence metrics in MEG and EEG data (Maris and Oostenveld, 2007; Maris et al., 2007). Our procedure for investigating changes in model parameters is shown schematically in Fig. 2 and is detailed in Algorithm 1.

Algorithm 1. Group-level nonparametric statistical test for each R-MFM parameter p_i

Null Hypothesis (H_0): $\mathbf{p_i}$ does not differ across the three assessments points

1. Collect $\mathbf{p_i}$ for all 73-channels across all subjects and assessments into a single super-set.
2. Randomly partition the super-set into three equal sets of subjects.
3. Calculate the cluster-based test-statistic as follows:

   a. For every channel, compare the parameter value $\mathbf{p_i}$ across the three assessment-points, using the corresponding F-test statistic.
   b. Select all channels with F-values larger than a given threshold.

Table 1

Initial values and physiologically restricted limits of model parameters in the current study as prescribed by Rowe et al. (2004a). The ten model parameters that were varied during data fitting are indicated with an asterisk (*) next to their initial values. The limits, fixed values, and initial values are in line with the independent sources and physiological measures (Robinson et al., 1997; Rowe et al., 2004b; Shwedyk et al., 1977; Van Boxtel, 2001).

Model	Parameter	Description	Physiological limits	Initial value
EEG parameters	γ_e	Cortical damping parameter to incorporate reduction in signal with increasing axonal distance	[40, 400]	130 per second*
	α	Dendritic decay rate parameter to incorporate temporal spread and conduction delay in the dendritic tree	[10, 200]	75 per second*
	β	Dendritic rise rate parameter to incorporate temporal spread and conduction delay in the dendritic tree	Depends on "α	$3.8 \times \alpha$ per second
	t_0	Conduction delay parameter to incorporate temporal delay in signal transmission from cortex to thalamic nuclei and back	[0.06, 0.13]	0.084 s*
	G_{ee}	Excitatory gain parameter to incorporate connection strength from pyramidal cells	[0, 50]	5.4*
	G_{ei}	Local intra-cortical inhibitory gain parameter to incorporate connection strength from stellate cells	[−35, −1]	−7*
	G_{ese}	First corticothalamocortical gain parameter to incorporate combined strength of connections from cortex to secondary relay nuclei and back to cortex	[0, 50]	5.6*
	G_{esre}	Second corticothalamocortical gain parameter to incorporate combined strength of connections from cortex to reticular nucleus to secondary relay nuclei of thalamus and back to cortex	[−30, 0]	−2.8*
	G_{srs}	Intrathalamic gain parameter to incorporate connection strength within two thalamic nuclei (TRN and SRN)	[−15, 0.5]	−0.6*
	$k_0 r_e$	Volume conduction filter parameter	Fixed	3.0 a.u.
	l_x, l_y	Linear dimensions of cortex	Fixed	0.5 m
	r_e	Characteristic pyramidal axon length	Fixed	0.08 m
	P_0	Overall power normalization	Estimated from the data	Estimated from the data*
EMG parameters	A	Power normalization	[0, 99]	0.5 μV²/Hz*
	f_{pk}	Peak frequency of the EMG spectrum	Fixed	40 Hz
	δ	Asymptotic slope parameter	Fixed	2 a.u.

c. Cluster the selected channels in connected sets on the basis of spatial adjacency.
d. Calculate the cluster-level F-statistic by taking a sum over all F-values within a cluster.
e. Output the largest of the cluster-level statistics.

4. Repeat Steps 2 and 3 a large number of times (e.g., 10,000) and construct a histogram of the test statistics.
5. Using the observed test-statistic and the histogram from Step 4, estimate the proportion of random partitions that resulted in a larger test-statistic than the observed test statistic. This proportion is the p-value.
6. If the p-value is less than the designated critical alpha-level ($p = 0.05$, corrected for False Discovery Rate), then conclude that the null hypothesis H_0 is rejected and that the parameter $\mathbf{p_i}$ is significantly different across assessment points.

Model extension 2: TRN connectivity

The original R-MFM, as described above, incorporates interactions between the cortex, reticular nucleus (TRN), and the specific relay nucleus (SRN) of the thalamus. However, it does not account for within-TRN interactions. One potential approach for modeling lateral connectivity in the TRN is to simulate and fit EEG power spectra concurrently across all EEG channels, an approach referred to as non-uniform R-MFM (O'Connor and Robinson, 2004; Robinson et al., 2003b). In this non-uniform approach, interactions between the modeled TRN cells can be retrieved after concurrent data simulation and fitting. The difficulty, however, is that in addition to fitting the 10 usual parameters per channel (see Table 1), simulating and fitting the coupled connectivity between 73 TRN cells (due to 73-channel EEG data) would come at the cost of increased computational resources and putative loss of analytical tractability in some cases (O'Connor and Robinson, 2004).

To address this challenge without resorting to a non-uniform modeling approach, we developed a novel procedure to model TRN's lateral connectivity and to explore changes in such connectivity associated with meditation training (Fig. 3). After model fitting of experimental spectra for all electrodes, white noise was injected into the modeled cortical cells (Fig. 3C). The activity due to the injected noise in the modeled TRN cells was extracted using linear algebra based on the original time domain R-MFM equations:

$$\phi_r(t) = \frac{\phi_e\left(t - \frac{t_0}{2}\right)[G_{esre} + G_{ese}G_{srs}] + \phi_n(t)[G_{es}G_{sn}G_{srs}]}{(G_{es}G_{sr})(1 - G_{srs})}, \quad (4)$$

where $G_{sn} = 1$, $G_{es} = \sqrt{G_{ese}}$, and $G_{sr} = \sqrt{|G_{srs}|}$. In order to analyze TRN connectivity, correlations between the extracted signals from TRN cells were computed (a high correlation between two TRN cells would indicate higher connectivity). For robust estimation, many iterations ($n = 100$) of noise injection and correlation matrix estimation were performed for each cell. The correlation matrix was then averaged over all trials and k-means clustering was performed on the resulting matrix. The value of k was chosen based on the visual inspection of the dendrogram generated by hierarchical clustering (MATLAB, 2010). Longitudinal changes in the structure and the connectivity of these clusters were evaluated using non-parametric statistical testing (Algorithm 1).

Stability analysis

Using linear stability analysis, Robinson et al. (2002) suggested that low-frequency instabilities of the brain can be modeled in a reduced three-dimensional parameter space < xyz >, where, $x = \frac{G_{ee}}{1 - G_{ei}}$, $y = \frac{G_{ese} + G_{esre}}{(1 - G_{srs})(1 - G_{ei})}$, and $z = -\frac{G_{srs}\alpha\beta}{(\alpha + \beta)^2}$. These parameters represent cortical (x), corticothalamic (y), and intrathalamic stability (z)), respectively. In their procedure, Robinson et al. (2002) defined the stability zone for the modeled brain as the < xyz > space under a three-dimensional surface defined by parameter values that induce instabilities in different frequency bands and features of the EEG (alpha, theta, and spindles). Thus, various brain states can be mapped onto this < xyz > space (see Fig. 3 in Robinson et al., 2002).
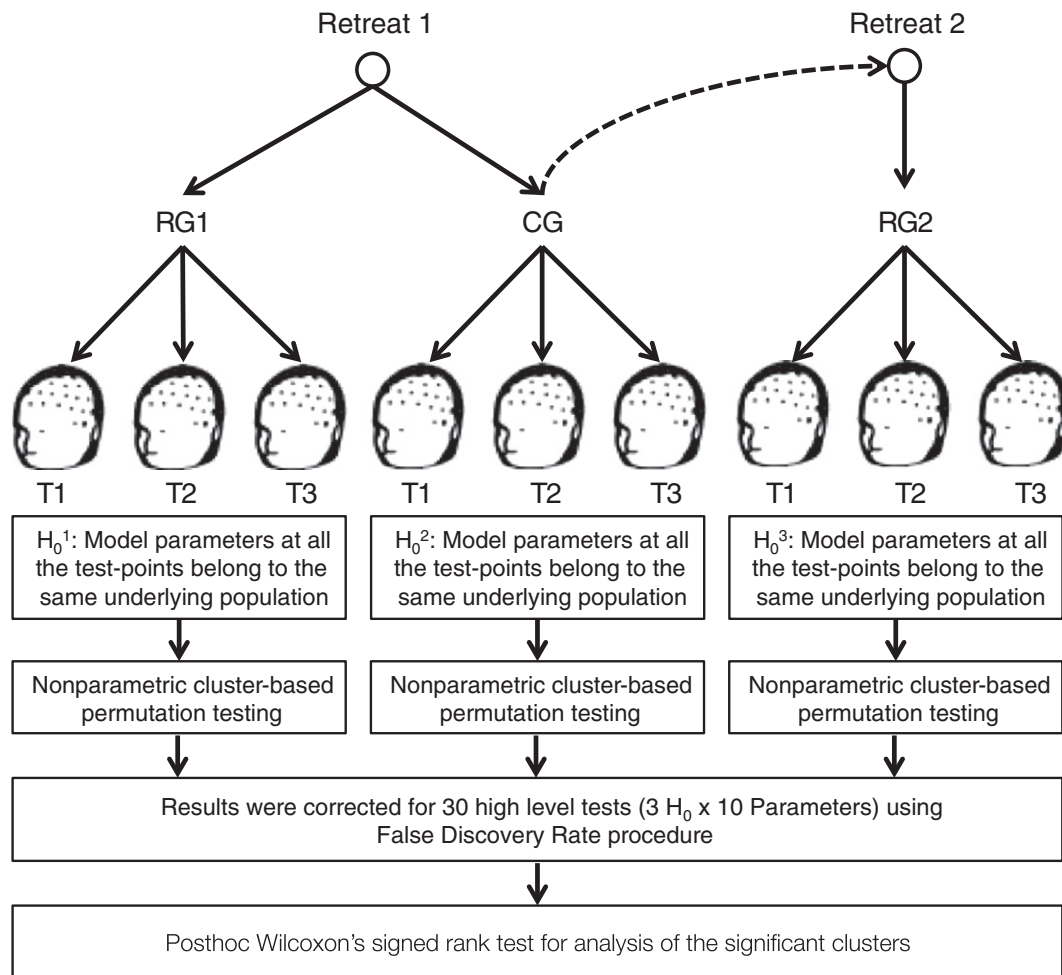
Fig. 2. Experimental design for longitudinal analysis of changes in model parameters due to training. After fitting the model for each assessment, the null hypotheses were tested for each group using the nonparametric cluster-based permutation analysis, followed by False Discovery Rate (FDR) correction for 30 nonparametric tests. The direction of effects, i.e. how parameter values change from T1 to T2 to T3, were examined with a Wilcoxon's test (with Bonferroni correction). Overall, this extension provides a statistical approach for longitudinal analysis of changes in the model parameters across all channels.

To explore how observed longitudinal changes in model parameters may alter the overall stability of modeled brain dynamics, fitted model parameters from the three assessment points were mapped to the reduced $< xyz >$ space separately for each retreat. As in the case of other model parameters, non-parametric statistical testing (Algorithm 1) was used to longitudinally analyze changes in the reduced-set of stability parameters (x, y, and z).

Results

All reported post-hoc Wilcoxon tests are Bonferonni-corrected (adjusted p-values reported, where indicated).

Data fitting

Using the LEV approach, experimental EEG power spectra were fitted independently for all electrodes (73 channels), separately for each participant and assessment point. As shown in Fig. 4, the model was successful in recreating the recorded EEG spectra (see Table 2 for goodness of fit results), while keeping the parameters within the physiologically plausible range (Tables 3 and 4). To verify that the aggregate model fitting procedure was unbiased across assessments, a non-parametric false-discovery-rate (FDR)-based procedure was used to find differences in the sum-squared errors in fit for each channel across the three assessments within each group of participants. Dependent

sample F-tests were used (with a Bonferroni-corrected alpha level of $p < 0.05$) to test for differences across assessments. No differences in fit accuracy were found across assessments in any group, demonstrating that the model fitting was generally unbiased.

Longitudinal analysis of model parameters

As expected, no changes in any of the 10 model parameters were found across assessments for the CG. Changes in two out of 10 parameters were found to replicate across retreats: intrathalamic gain (G_{srs}) and cortico-thalamic delay (t_0). In RG1, a decrease in intrathalamic gain was found in the right lateral parieto-occipital cluster of modeled channels ($p = 0.01$, FDR corrected; Fig. 5). Bonferroni-corrected (.05/3) post-hoc Wilcoxon tests revealed a significant reduction at T2 ($p < 0.001$) and T3 ($p = 0.007$), as compared to T1. No differences were found between T2 and T3. In RG2, a similar pattern of decrease in intrathalamic gain was found in a right-parietal cluster of modeled channels ($p = 0.04$; Fig. 5). Post-hoc Wilcoxon tests revealed a reduction in intrathalamic gain at T2 ($p = 0.014$) and T3 ($p = 0.001$), as compared to T1. Again, no difference was found between T2 and T3.

The cortico-thalamic delay parameter increased with meditation training (Fig. 6). This effect was evident in both retreat groups. In RG1, an increase in the delay parameter was found at bilateral parietal–occipital model locations ($p = 0.003$). Wilcoxon tests revealed a significant increase at T2 ($p < 0.001$) and T3 ($p = 0.007$) when compared to
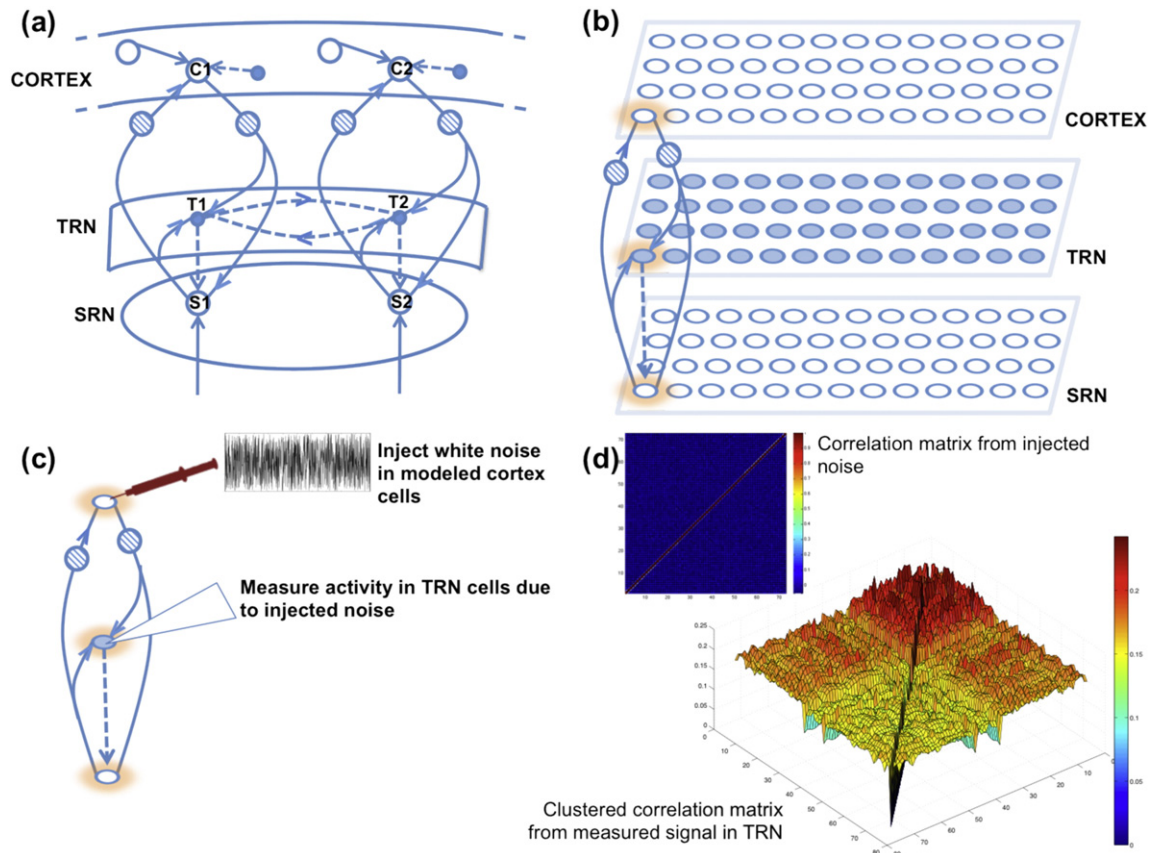
Fig. 3. Measuring interactions in the modeled TRN layer. (a) Two units of the model and their interactions (dashed lines) in the TRN layer are shown. Ideally, parameter values for such interactions should be fitted along with all the other parameters of the model. However, given 73 units in total, this approach will lead to a combinatorial explosion of the fitting procedure. Thus, we developed a novel approach as described in (c). (b) The three layers of the model. Each column is modeled independently using the LEV approach. (c) The procedure formalizing within-TRN connectivity. After fitting the model to real EEG data, white noise was injected in the cortical cells and the resulting activity in the TRN cells was measured. Connectivity analysis in the TRN layer was then performed. (d) An example correlation matrix of injected white noise (no off-diagonal correlations present) and the resulting correlation matrix from TRN cells for a representative participant are shown. The diagonal elements in the TRN layer are set to zero for clarity. Instead of random ordering, an organized structure is evident in the correlation matrix of TRN cells, suggesting that even though these cells were modeled independently, connectivity information between them can still be discovered.

T1 and no change between T2 and T3. Similarly, in RG2, an increase was found at right parietal–occipital modeled locations ($p = 0.01$). Wilcoxon tests revealed an increase in delay parameter value at T2 ($p = 0.001$) and T3 ($p = 0.001$) when compared with T1, but no change was found between T2 and T3.

Stability analysis

To examine changes in stability of the modeled EEG dynamics in a reduced three-dimensional parameter space, the cortical (x), corticothalamic (y), and intrathalamic (z) stability parameters were analyzed separately. Only the intrathalamic stability parameter z was found to change across assessments for both retreat groups (RG1: p (FDR corrected) $= 0.011$ and RG2: $p = 0.033$; Fig. 7). The cluster locations found for z were identical to those found for G_{srs}. This is because the z parameter, by definition, is directly proportional to G_{srs}, which changed significantly as indicated in the section Longitudinal analysis of model parameters. No cluster was found for the CG. Therefore, for the purpose of analysis, clusters found for RG1 participants were used to extract data for post-hoc comparisons of CG participants within Retreat 1, while clusters found for RG2 were used to extract CG data within Retreat 2. Thus, for Retreat 1 control data, CG cluster electrodes were not based on the clusters found for these individuals themselves when in their own retreat. A Wilcoxon test for the RG1 model cluster revealed a significant decrease in z at T2 ($p = 0.002$) and at T3 ($p = 0.001$), as compared to T1. As expected, there were no changes in z parameter values for the corresponding cluster extracted from the modeled CG

data. A Wilcoxon test for this cluster in the RG2 model revealed a significant decrease in the z parameter at T2 ($p = 0.014$) and T3 ($p = 0.001$), when compared to T1. Again, there was no change in z values extracted from CG for the same cluster.

TRN connectivity analysis

We used the second model extension (see Model extension 2: TRN connectivity) to examine longitudinal changes in intra-TRN connectivity. We took a three-part approach to this analysis. First, to qualitatively examine the overall pattern of intra-TRN connectivity, we used k-means clustering to identify two groups of TRN cells characterized by high within-cluster correlations. To visualize the topography of these k-means clusters, we utilized the topographical organization of the experimentally recorded EEG, where each of the channels is an independently modeled instance of R-MFM (see example in Fig. 8a). Within the TRN layer, each cell in the anterior cluster was assigned $+1$ and each cell in the posterior cluster was assigned -1. To create average "scalp" cluster topographies, we averaged these $+/-1$ assignments across participants within each dataset and assessment. Overall, we observed an anterior to posterior segregation of within-TRN layer connectivity that is visualized at the group level in Fig. 8b.

Next, we investigated longitudinal changes in this anterior/posterior-segregated pattern. We used nonparametric cluster-based permutation testing on the topographies created from anterior/posterior assignments based on inter-cell correlation values. No significant changes were found across assessments for any group, indicating that
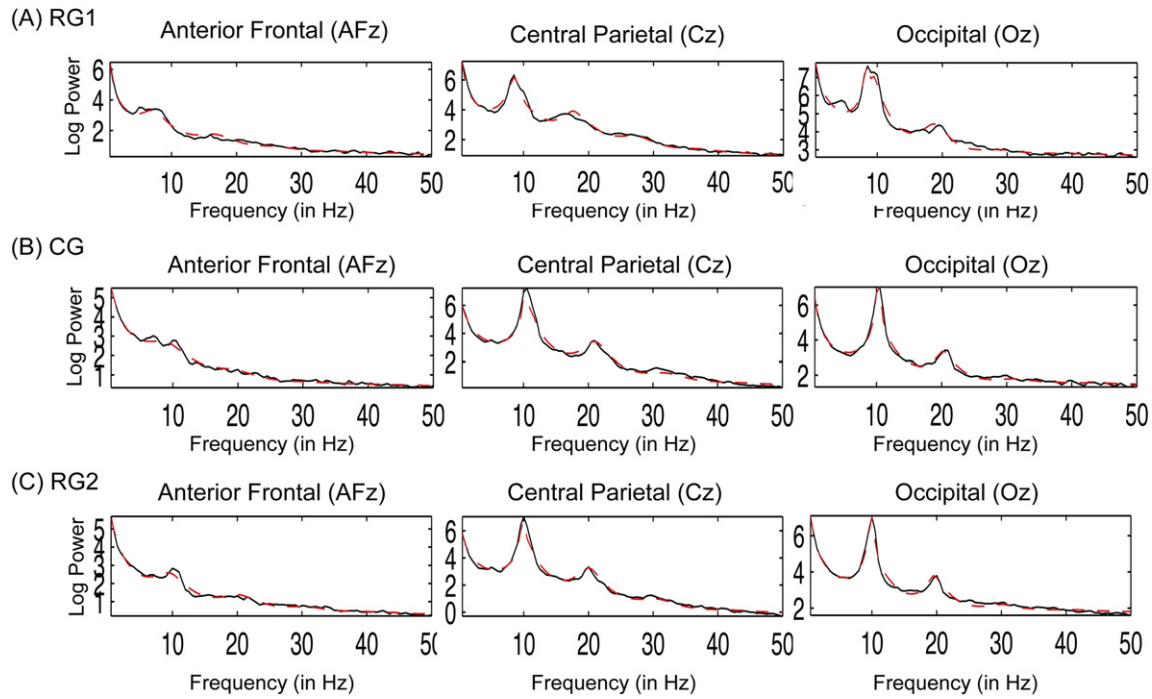
Fig. 4. Results from model fitting of the EEG data for representative participants across scalp and groups. Real EEG spectrum is shown in solid black line and modeled EEG spectrum in dashed red line. Each column shows a different mid-line channel across the scalp (out of 73 channels, due to space limitations). There is close correspondence between the model spectra and experimental spectra across the scalp, participants, and groups.

this feature of spatial segregation is stable with respect to shamatha and related FA-meditation training.

Finally, to examine longitudinal changes in connectivity (i.e., mean correlation values) both within and between the anterior and posterior clusters, we performed a related-samples Friedman's Analysis of Variance by Ranks Tests (a non-parametric alternative to parametric one-way ANOVA with repeated measures Friedman, 1937) separately for the three participant datasets (RG1, CG, and RG2). For each dataset, we examined the null hypothesis that the distributions of within- and between-cluster connectivity did not differ across time points. Out of the nine tests (i.e., 3 datasets × 3 connectivity tests (2 within-cluster and 1 between-cluster)), only two rejected the null hypothesis (FDR-corrected $p < 0.05$), such that in both retreat groups (RG1 and RG2) between-cluster connectivity was significantly different across time points (FDR-corrected $p = 0.0495$ for each dataset). In RG1, the post-hoc Wilcoxon tests revealed a significant increase in between-cluster connectivity at T3 as compared to T1 ($p = 0.046$), and no significant difference was found between T1 and T2 or between T2 and T3 (Fig. 8c). In RG2, however, a significant increase in between-cluster connectivity was observed at T2 ($p = 0.010$) compared with T1, (Fig. 8c) and no differences were found between T1 and T3 or between T2 and T3 (Fig. 8c).

Table 2
Goodness of fit results based on R-square values. The results are averaged over all channels and participants for each assessment and group, after fitting to the real EEG spectrum. Overall, the model accounted for more than 98% variance in all the cases. More importantly, low standard deviations indicate that the model fit the data consistently across the scalp and the participants.

	RG1		CG		RG2	
	μR^2	σR^2	μR^2	σR^2	μR^2	σR^2
T1	0.985	0.0055	0.984	0.0053	0.983	0.0063
T2	0.983	0.0076	0.985	0.0057	0.984	0.0057
T3	0.984	0.0061	0.985	0.0063	0.983	0.0069

Relating changes in model parameters to observed cortical activity

A series of regressions were used to examine relations between changes in model-derived parameters and previously reported longitudinal changes in beta-band power and alpha-frequency in this same dataset (Saggar et al., 2012). Because patterns of change in model parameters and observed oscillatory activity were similar across retreats, RG1 and RG2 datasets were combined for the regression analyses.

Relating changes in model parameters to change in beta-band power

Neither the intrathalamic gain nor the corticothalamic delay at T1 was a significant predictor of beta-band power at T1 ($R^2 = 0.01$, $F(1,42) = 0.028$, $p = 0.867$ and $R^2 = 0.013$, $F(1,42) = 0.565$, $p = 0.456$, respectively).

We examined whether longitudinal changes in these two model parameters might predict reductions in observed beta-band power. In the first multiple regression, beta-band power and intrathalamic gain at T1 were included as predictors of beta-band power at T3 to account for baseline levels in these predictors prior to training. These predictors explained a significant amount of variance in T3 beta-band power ($R^2 = 0.80$, $F(2,41) = 84.22$, $p < 0.001$). In the second step, the addition of the intrathalamic gain parameter value at T3 did not significantly add to the explained model variance ($\Delta R^2 = 0.001$, $\Delta F(1,40) = 0.21$, $p = 0.65$).

In a second multiple regression, we used an identical analytic strategy to test the predictive effects of corticothalamic delay on observed beta-band power. Again, beta-band power at T3 served as the dependent variable and beta-band power and corticothalamic delay at T1 were included as initial predictors. These predictors explained a significant amount of variance in T3 beta-band power ($R^2 = 0.80$, $F(2,41) = 83.35$, $p < 0.001$). Similar to the first hierarchical regression, the addition of T3 corticothalamic delay value did not significantly add to the explained model variance ($\Delta R^2 = 0.002$, $\Delta F(1,40) = 0.45$, $p = 0.51$). Altogether, collapsed across the retreats, changes in observed beta-band power were not predicted by longitudinal changes in either the model-predicted intrathalamic gain or corticothalamic delay parameters.

Table 3

Mean values of fitted model parameters for each set of participants (RG1, CG, and RG2) and assessments (T1, T2, and T3). The values are averaged over all channels and participants after fitting to the real EEG spectrum collected during meditation state. As evident, the final parameter values are within the physiologically plausible range (refer to Table 1).

		α	t_0	G_{srs}	γ_e	G_{ee}	G_{ei}	G_{esre}	G_{ese}	p_0	A
RG1	T1	113.7	0.0889	-0.8977	282.7	24.5	-29.93	-4.99	15.12	0.1652	7.8
	T2	116.9	0.0865	-0.8027	287.1	24.7	-30.34	-3.73	14.48	0.1468	6.8
	T3	113.8	0.0860	-0.8471	287.9	24.0	-30.10	-3.94	15.54	0.1694	7.2
CG	T1	112.0	0.0863	-0.9474	275.6	24.0	-29.89	-3.86	16.31	0.2702	8.1
	T2	113.2	0.0850	-0.9288	281.8	25.0	-30.75	-3.64	15.04	0.2117	7.9
	T3	111.2	0.0850	-0.9295	273.6	23.9	-29.87	-3.81	16.38	0.2508	7.6
RG2	T1	111.6	0.0913	-0.8419	296.1	25.5	-30.68	-4.95	15.50	0.2244	9.4
	T2	112.4	0.0897	-0.8046	293.9	26.1	-31.16	-4.35	15.02	0.2051	8.9
	T3	114.6	0.0896	-0.8030	287.8	25.8	-30.26	-4.72	14.83	0.1937	8.9

Relating changes in model parameters to change in individual alpha frequency

Intrathalamic gain marginally predicted IAF at T1 ($R^2 = 0.08$, $F(1,42) = 3.62$, $p = 0.064$), while corticothalamic delay at T1 significantly predicted IAF at T1 ($R^2 = 0.50$, $F(1,42) = 42.67$, $p < 0.001$).

We next examined whether longitudinal changes in the two model parameters could explain the longitudinal reduction in IAF. Intrathalamic gain at T1 explained a significant amount of variance in T3 IAF ($R^2 = 0.87$, $F(2,41) = 138.65$, $p < 0.001$). The addition of the T3 intrathalamic gain parameter did not significantly add to the explained model variance ($\Delta R^2 = 0.006$, $\Delta F(1,40) = 1.9$, $p = 0.175$).

In a second multiple regression, we again included IAF at T3 as the dependent variable and IAF and corticothalamic delay at T1 as predictors to account for baseline levels before training. These predictors explained a significant amount of variance in T3 IAF ($R^2 = 0.87$, $F(2,41) = 137.73$, $p < 0.001$). Contrary to the prior analyses, the addition of the T3 corticothalamic delay value significantly improved the explained model variance ($\Delta R^2 = 0.042$, $\Delta F(1,40) = 19.16$, $p < 0.001$). Altogether, collapsed across the retreats, reductions in IAF were associated with increases in the corticothalamic delay parameter ($\beta = -0.46$).

Discussion

This paper presents the first mean-field computational model of scalp-measured electrophysiology obtained during the practice of focused attention meditation. By simulating and fitting EEG data recorded during meditation, this approach permits mathematical analysis of longitudinal changes in oscillatory activity and makes testable predictions to advance experimental research in this area. The mean-field modeling approach of Robinson et al. (2001b) was used to simulate scalp-recorded EEG with the incorporation of corticocortical, corticothalamic, and intrathalamic loops. This model was successfully extended to allow for longitudinal analysis of changes in model parameters and intra-TRN connectivity due to training. We observed reliable training-related changes in two model parameters, replicated for each of two separate training groups. First, the intrathalamic gain parameter (G_{srs}) decreased significantly with training, suggesting reduced inhibition of modeled

SRN cells by the TRN. Using stability analysis, we found that the reduction in intrathalamic gain provided increased stability to the modeled dynamical system. Second, the corticothalamic delay parameter (t_0) increased with training, indicating an increase in transmission delay between modeled cortical and thalamic cells. The increase in modeled corticothalamic delay strongly predicted individual reductions in experimentally observed individual alpha frequency (Saggar et al., 2012). Lastly, intra-TRN connectivity analysis implicated a clear anterior–posterior connectivity-based segregation in the modeled TRN layer. While this anterior–posterior connectivity remained stable over training assessments, an increase in between-cluster anterior–posterior connectivity was observed in both retreat groups following training. Taken together, these findings suggest that changes in attentional and other cognitive processes through intensive meditation training may be supported by longitudinal changes in corticothalamic dynamics.

Modeling dense-array EEG with ER-MFM

To minimize the effect of local dependency at low frequencies, we restricted the analysis to frequencies higher than 2 Hz. Further, two specific methods were used to minimize the local dependence effects at the alpha frequency. First, during preprocessing, EEG data were transformed using scalp current density (SCD) estimation. The SCD transformation creates reference-free EEG and reduces effects of volume conduction (Srinivasan et al., 2007), thereby lowering the effect of distant activity on local sites. Second, we used a nonparametric cluster-based permutation approach to identify longitudinal changes in model parameters. This cluster-based approach is similar to cluster-corrected algorithms used in fMRI data analysis, where information from neighboring voxels is considered when estimating the activity at a local site (Smith and Nichols, 2009). This approach, although insensitive to extremely local changes (e.g., when studying effects at the single scalp electrode level), works well for EEG data (Maris and Oostenveld, 2007). Thus, by including information about neighboring sites, this cluster-based extension helps to minimize violation of local independence and likely provides a more plausible model than the LEV approach alone. In the future, this approach should be tested against

Table 4

Average standard deviation values of fitted model parameters for each set of participants (RG1, CG, and RG2) and assessments (T1, T2, and T3).

		α	t_0	G_{srs}	γ_e	G_{ee}	G_{ei}	G_{esre}	G_{ese}	p_0	A
RG1	T1	13.53	0.0047	0.4006	57.31	3.09	2.07	2.53	4.14	0.1384	4.09
	T2	13.9	0.0056	0.2812	49.51	3.17	2.4	2.72	4.92	0.1245	3.69
	T3	13.03	0.006	0.3318	52.82	4.04	2.32	3.01	4.92	0.1552	4.37
CG	T1	11.21	0.0066	0.4187	55.6	2.77	2.05	2.01	4.62	0.191	2.91
	T2	11.27	0.0072	0.4193	62.91	3.25	2.55	2.5	6.22	0.1578	2.89
	T3	11.12	0.0064	0.4239	60.13	3.61	1.99	2.22	6.31	0.1849	2.64
RG2	T1	10.9	0.0059	0.3918	65.96	3.16	2.12	2.84	5.14	0.1696	4.13
	T2	9.44	0.007	0.3619	66.38	3.54	2.9	2.71	5.39	0.1566	3.71
	T3	9.94	0.0077	0.3691	64.37	3.63	2.89	2.63	4.18	0.1687	3.81
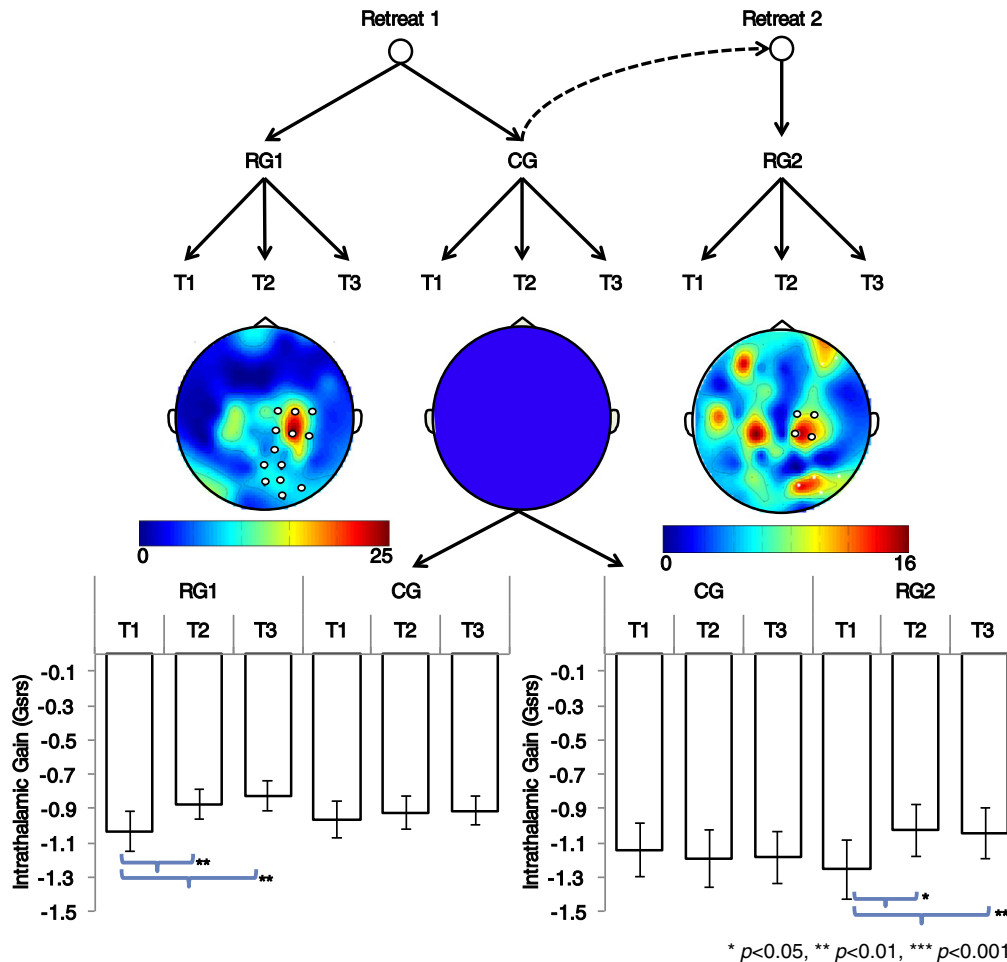
Fig. 5. Reduction in intrathalamic gain (G_{srs}) during meditation. The color bars represent F-statistics. Using a nonparametric cluster-based permutation approach, significant clusters were found in RG1 and RG2, whereas no clusters were found in CG. Clusters from RG1 and RG2 were used to extract data from CG participants, separately for each retreat, for post-hoc comparison and plotting of bar graphs. Overall, the reduction in intrathalamic gain during meditation was replicated across the retreats in similar spatial locations and no effect was found for the CG using either cluster. Error bars represent standard error of the mean.

more sophisticated modeling approaches, where inter-connectivity between channels is also modeled (O'Connor and Robinson, 2004; Robinson et al., 2003b).

After fitting the experimental EEG data, the R-MFM model was able to explain more than 98% of the variance across channels, assessments, and groups (Table 2). Here, SOBI and SMART were used to ensure that only high-quality EEG, relatively free from EMG and EOG contamination, was used for model fitting (Saggar et al., 2012). This likely contributed to the success of fitting the model to the recorded data. It is possible, however, to further improve accuracy with more sophisticated fitting algorithms. For example, Kerr et al. (2011) used Monte Carlo simulations to enable multiple random initializations for data fitting, thereby reducing potential bias that can be introduced when initial parameter values are held fixed.

Longitudinal changes in intrathalamic gain

Following training, we observed a reduction in the amplitude of intrathalamic gain in the modeled EEG sites overlying the right parietal region in both retreat groups. Compared to pre-training values, intrathalamic gain was reduced by the mid-assessment point and remained low at post-assessment. This parameter represents the strength of inhibitory connection between the TRN and SRN cells. Because TRN cells exert a solely inhibitory influence on the SRN in this model, the observed reduction in this parameter suggests decreased inhibition of SRN cells.

The TRN has long been hypothesized to play important roles in both selective attention (Crick, 1984) and general alertness (Steriade et al., 1993). Crick (1984) argued that, during selective attention, TRN cell activity modulates the corticothalamic inputs that excite or inhibit specific SRN cells, thereby regulating the flow of sensory information to the cortex. This hypothesized modulation of SRN cells is assumed to form a reciprocal relation between the activity of TRN and SRN cells. In recent work, McAlonan et al. (2008) provided direct evidence for this reciprocal relation by demonstrating that TRN cells serve as an initial source of modulation in SRN cells (McAlonan et al., 2008). In another study, Lam and Sherman (2011) reported that a surprising percentage (~25%) of the recorded neurons from somatosensory TRN received non-topographic input from all three somatosensory relay nuclei of the thalamus (i.e., posterior medial, ventroposterior medial, and ventroposterior lateral relay nuclei), suggesting that some subpopulations of TRN neurons may integrate somatosensory inputs from different thalamic relays. The authors argued that, consistent with Crick's hypothesis, such integration in TRN allows for competition between different inputs at the thalamic level itself, allowing stronger and more salient inputs to suppress weaker and less relevant inputs. Altogether, these and other related studies (Jones et al., 2010; Lam and Sherman, 2010), provide evidence for TRN's complex and versatile role in tuning sensory inputs to enable salient information to reach the cortex.

Regarding the role of TRN in general alertness, Halassa et al. (2011) used optogenetics and multi-electrode recording in awake behaving as well as sleeping mice to selectively and causally test the role of the TRN
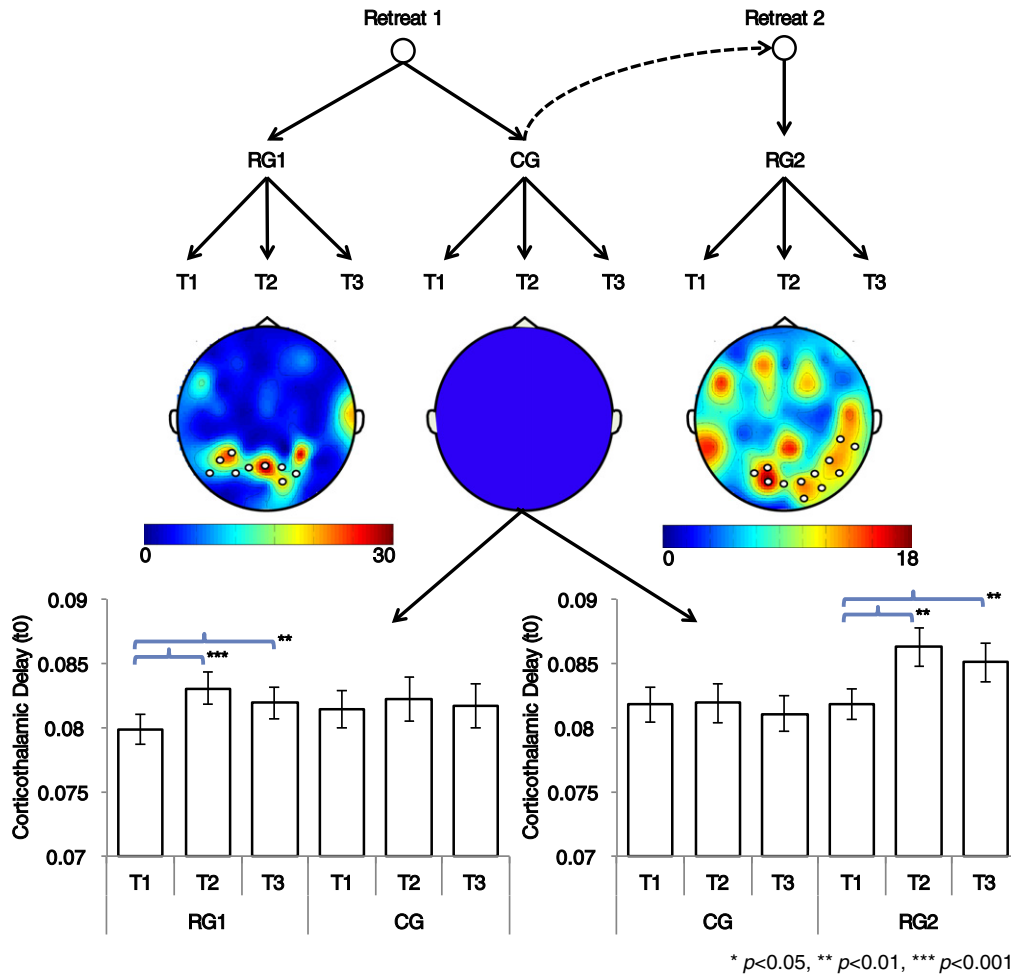
Fig. 6. Increase in corticothalamic delay (t_0) during meditation. The color bars represent F-statistics. No clusters were found in the CG. Clusters from RG1 and RG2 were used to extract data from CG participants, separately for each retreat, for post-hoc comparison and plotting of bar graphs. Overall, increased cortico-thalamic delay was found in parietal–occipital regions, in both retreat groups, at the middle and the end of the retreat. Error bars represent standard error of the mean.

in thalamic bursting and subsequent generation of neocortical spindles. The authors reported that optogenetic activation of TRN resulted in sleep-like spindles and that induction was state dependent and was evident largely during non-rapid eye-movement (NREM) sleep and somewhat during wakefulness, but not at all during rapid eye-movement (REM) sleep (Halassa et al., 2011).

Taken together, this overview of TRN findings suggests that the reduction in amplitude of the intrathalamic gain parameter (or inhibition by TRN cells) is consistent with the notion that, following intensive training, practitioners may be more focused and alert when engaged in meditation. This model-generated hypothesis provides some new insight into the brain processes potentially associated with meditation
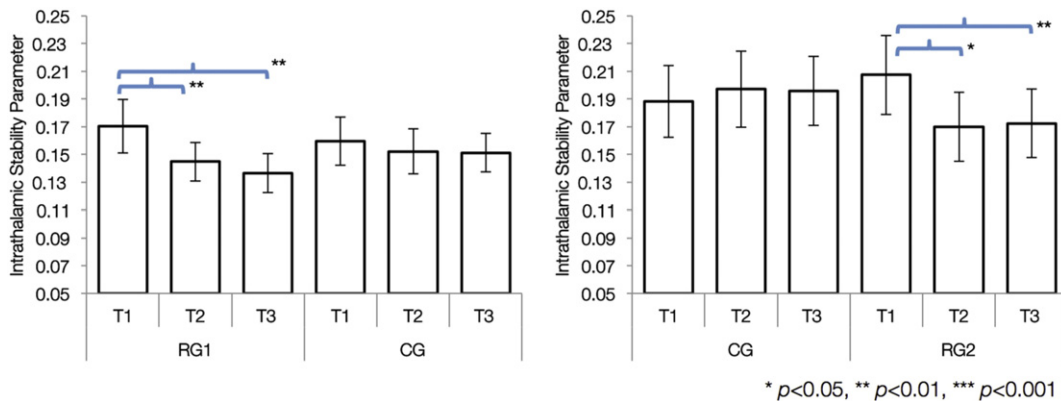
Fig. 7. Stability analysis during meditation. The bar chart depicts a significant drop in intra-thalamic stability parameter (z) in both retreat groups, suggesting increased stability as a result of training. No changes were found in the CG. Error bars represent standard error of the mean.
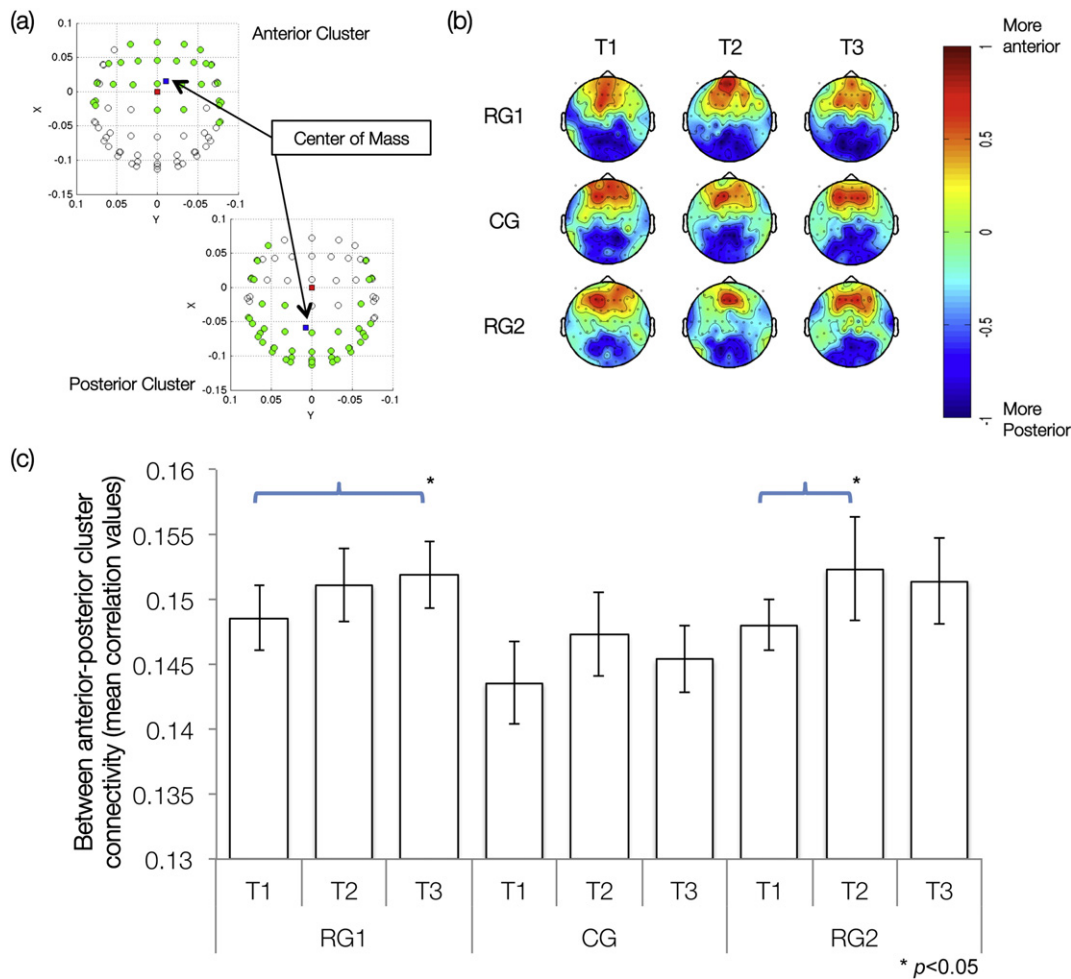
Fig. 8. Connectivity analysis of the TRN layer. (a) Representative single participant posterior and anterior clusters, found after k-means clustering on the correlation matrix of TRN cells. (b) Average topographical maps (over all participants) for each assessment and group are shown during the meditation state. For each participant, each channel was given a value of + 1 (when in the anterior cluster) or − 1 (when in the posterior cluster). Overall, clear separation between the anterior and poster regions of the modeled TRN was found. (c) Between clusters connectivity analysis revealed increased connectivity between anterior and posterior clusters associated with meditation training. Error bars represent standard error of the mean.

training. Specifically, modulation by the TRN cells could be responsible for enhanced cortical activity for efficient processing of salient stimuli (i.e., object of focus) during meditation. In support of this hypothesis, we have observed decreased bilateral frontocentral EEG beta activity ($1.2 * IAF$ to 30 Hz) in this same cohort of participants during practice of FA meditation. Reduced beta activity suggests increased activation of fronto-parietal attention networks with increased training in these techniques (Saggar et al, 2012). Behavioral evidence further indicated improved performance on tasks assessing visual perception, vigilance, and response inhibition for this cohort following training (MacLean et al., 2010; Sahdra et al., 2011). In order to directly examine the significance of the intrathalamic gain parameter for models of enhanced attention and alertness, future work should examine whether similar patterns of change in model parameters are observed during performance of sustained attention and response inhibition tasks.

Interestingly, using a similar computational model based on only nine EEG electrodes, Rowe et al. (2005) showed that the baseline intrathalamic gain parameter is reduced in adolescents diagnosed with attention-deficit hyperactivity disorder (ADHD) after stimulant medication. Hence, our modeling results can serve to motivate further study of shamatha and focused-attention meditation as part of a treatment approach for patients with ADHD. Preliminary support for the efficacy of meditation training in individuals with ADHD has already been shown in several recent studies incorporating regular practice of FA meditation as a part of training (Mitchell et al., 2013; Zylowska et al., 2008, 2009). Zylowska et al. (2008) conducted a study that included

both adolescents and adults with ADHD and reported post-training improvements in self-reported scores on ADHD, depression, and anxiety symptoms, as well as behavioral performance on attention regulation tasks. Further, these improvements were sustained at a 3-month follow-up (Zylowska et al., 2009). In a recent pilot study, adults with ADHD improved in self-reported and clinician ratings of ADHD, as well as task-based executive functioning scores, following an 8-week group-based meditation training, as compared to a randomized wait-list control group (Mitchell et al., 2013).

Longitudinal changes in corticothalamic delay

A corticothalamic delay parameter was incorporated in the model to represent the conduction delay in signal transmission both from the cortex to thalamic nuclei and from thalamic nuclei to the cortex. It is important to note that neither the R-MFM nor the extended model presented in this paper presumes the existence of cortical or subcortical pacemakers or "clocks" to generate periods of alpha and beta rhythms. Instead, the corticothalamic delay itself facilitates emergence of alpha and beta rhythms on the modeled scalp. Further, keeping all the other model parameters constant, the main effect of increasing the corticothalamic delay results in reduced alpha and beta frequencies (Robinson et al., 2001a; Saggar, 2011). Individual differences in this delay are also conjectured to contribute to the widely observed finding of individual differences in alpha frequency (IAF) values (Robinson et al., 2001b). Other, more recent, computational approaches have

shown that the corticothalamic feed-forward vs. feedback delay (i.e. asynchronicity) results in the emergence of surface-recorded alpha/beta rhythms without using explicit pacemakers (Jones et al., 2009; Kerr et al., 2013). Thus, there appears to be a strong basis for relating longitudinal changes in the modeled corticothalamic delay parameter to previously reported findings of lowered IAF in these same participants (Saggar et al, 2012).

The model architecture used in this paper appears to replicate critical aspects known from neurophysiological observation of the neuronal basis of alpha/beta rhythm generation resulting from thalamocortical interactions. For instance, to understand the neural basis of alpha-rhythm generation, Bollimunta et al. (2011) recently concluded that the alpha generators in layer 6 of the macaque primary-visual cortex were consistently the strongest contributors to alpha-rhythm generation across other penetrations. This observation, along with previous results showing that feedback from the striate cortex to thalamic nuclei originates from layer 6 of the same cortical column that receives afferents from the thalamic nuclei (Callaway, 1998; Sherman and Guillery, 2006), supports the idea that the alpha rhythm recorded over primary visual cortex of macaques could be generated primarily by thalamocortical interactions (Bollimunta et al., 2011).

Here, we observed an increase in the model parameter representing corticothalamic delay in modeled electrodes overlaying parietal–occipital regions. The increase in corticothalamic delay was observed across both training groups, and was evident at both the mid- and post-assessment points. Importantly, the increase in modeled delay values predicted a drop in observed alpha frequency (IAF values) after training. Studies of meditation, including our previous work (Saggar et al., 2012), have repeatedly shown that long-term meditators have reduced alpha frequency during meditation (Banquet, 1973; Kasamatsu and Hirai, 1966; Wallace, 1970; Zhang et al., 1988) as well as during baseline rest (Aftanas and Golosheikin, 2001, 2002, 2003). However, the biological basis for this finding is still unknown.

The present modeling results suggest that the increased corticothalamic delay involving parietal–occipital regions might account for the reduced alpha frequency observed in meditators. However, the construct of "corticothalamic delay" itself is complex. Multiple potential processes can influence corticothalamic effective delay. These include variable synaptic delays, activation of different subpopulations of pyramidal cells, interareal activation sequences, and changes in axonal and dendritic cable properties due to myelination variations (Meeren et al., 2002). Further, in addition to corticothalamic delay, changes in axonal conductance and decay time (anesthesia induced) have also been reported as a putative cause for reduced alpha (or dominant) frequency (Ching et al., 2010; Englehardt et al., 1991; Nunez, 1995). Additionally, changes in the dendritic decay rate have also been shown to affect alpha frequency (Robinson et al., 2001b). As no longitudinal changes were observed in the dendritic decay rate parameter, changes in the corticothalamic delay parameter seem the most viable candidate for reduction in alpha frequency following meditation training. However, it is unclear as to why an increase in posterior corticothalamic delay might occur with intensive meditation training.

One conjecture regarding the functional consequences of the increased corticothalamic delay is to facilitate sustained attention on incoming sensory or tactile stimuli with increased meditative expertise. This idea is based upon the argument that an increased delay will facilitate a subsequent increased asynchrony between the firing rates of the cortical and thalamic cells, potentially disrupting ongoing corticothalamic synchronization. In line with this argument, similar asynchronous inputs have been shown to be responsible for weakening previously strengthened inputs in the hippocampal cells in rats (Csicsvari et al., 2003; Huerta and Lisman, 1995). Given the regulatory role of TRN, the transient disruption of corticothalamic synchronization may enable increased effective SRN-based activation of cortex and thus modulate the initial processing of sensory inputs.

Stability analysis

Nonlinear instabilities or bifurcations in large-scale dynamical systems have been of wide interest to computational scientists. A sudden change in large-scale dynamical systems activity is considered to be a bifurcation (e.g., a transition from laminar to turbulent fluid flow is a common example of such change; Breakspear et al., 2006). Due to their disruptive nature for brain function, it is especially important to study such instabilities in neural dynamics (e.g., onset of seizure; Le Van Quyen et al., 2003; Mirowski et al., 2009). Robinson et al. (2002) extensively explored the dynamics of their R-MFM approach and observed that the model had only a few key instabilities that result in nonlinear behaviors. Of these instabilities, the first two (known as slow-wave and theta) lead to spike-wave nonlinear limit cycles in the slow-delta and fast-theta ranges, respectively. The other two instabilities (spindle and alpha peak) lead to a limit cycle with frequencies in alpha band range (~10 Hz). The spindle instability is of particular interest to our work as it originates in the intrathalamic loop (where we observed effects of meditation training) and spreads to the cortex due to thalamocortical projections (Breakspear et al., 2006; Robinson et al., 2002).

Using the reduced 3-d stability space, we observed that participants in both retreat groups had a significantly lower z-coordinate (representing intrathalamic stability) following training. This suggests that retreat participants' modeled brain state was further below the intrathalamic instability boundary (or tent's surface in z direction) after training. This decrease in the z-coordinate value is likely due to the observed decrease in the model's intrathalamic gain after training (see the section Stability analysis).

Although the participants in this study were neurologically healthy individuals, increased distance from the modeled intrathalamic instability boundary due to meditation training provides a fascinating motivation to further study shamatha and related focused-attention meditation as part of potential treatment strategies for epileptic patients. Recent reviews of psychobehavioral interventions for persons with epilepsy conceptualize interictal periods as a time-varying pattern of changing proximity to seizure boundary conditions (Tang et al., 2014). Thus, even modest improvements in stability, such as those reported here, may become critical in delaying or preventing seizure onset when an individual approaches the seizure boundary.

Connectivity in TRN layer

To model intra-TRN connectivity, a novel computational procedure allowed us to explore the connectivity structure without fitting a myriad of additional model parameters. Using this method, a clear frontoparietal functional division was observed in the modeled TRN layer. Interestingly, the discovery of a functional division in the modeled TRN layer is in line with animal studies where the afferent cortical connections to TRN layer are shown to be topographically structured (Zikopoulos and Barbas, 2007). Although this functional division was stable across time points, an increase in anterior–posterior between-cluster connectivity associated with meditation training was observed in both retreat groups. This effect was only evident for the post time point in RG1 and for the middle time point in RG2. One plausible reason for lack of consistency across retreats could be the small sample size of our study.

Using animal models, it has been well established that the cortical and thalamic afferents to the TRN are topographically organized (Crabtree and Killackey, 1989). Along the rostrocaudal axis, centroposterior loci in TRN receive afferents from the somatosensory, visual, and auditory cortices and their associated thalamic relay nuclei. Recent work by Zikopoulos and Barbas (2006), however, has provided novel evidence of strong prefrontal projections in the anterior sector of TRN. These authors have claimed that these prefrontal projections, although concentrated in the anterior TRN sector, are widespread and overlap extensively with the afferent projections from other cortical

and thalamic pathways in the TRN (Zikopoulos and Barbas, 2006). Additionally, the overlap between prefrontal and other cortical/thalamic projections in the TRN is thought to contribute to attentional selection of salient stimuli and attentional regulation (Zikopoulos and Barbas, 2007).

In light of this research, it could be speculated that the increase in connectivity between the anterior and posterior clusters in the modeled TRN layer following meditation training could be due to increased prefrontal projection strength on the TRN layer. This may reflect a putative mechanism for facilitating sustained attention on the incoming sensory/tactile breath stimulation. In this same cohort of participants, enhanced attention regulation as evidenced by improved response inhibition (presumed to be a frontally-mediated component of executive control) was observed following meditation training (Sahdra et al., 2011). Utilizing the ER-MFM model extension, future research can investigate this hypothesis by modeling EEG data collected while participants are engaged in an attention regulation task.

Limitations

Several limitations should be discussed. Our modeling approach was restricted to cortico-cortical, cortico-thalamo-cortical, and intrathalamic interactions. While these interactions are known to efficiently capture the general context of arousal and attention regulation, activity in other subcortical areas (e.g., the hippocampus and amygdala) are also known to be modulated during meditation practice (for a recent review, see Fox et al. (2014)). Future studies could examine whether the approach taken here can be adapted to include additional subcortical areas and associated interactions. This model may therefore be further extended to better understand the hypothesized mechanisms underlying shamatha and FA meditation practice and training.

Several factors unrelated to meditation training could have also contributed to the present findings. First, both retreats took place in a remote wilderness setting, where participants spent a majority of their time in solitary meditation. The environmental and acute behavioral changes associated with substantial time in solitary meditation likely exerted a number of non-specific effects. These could have manifested as observed physiological changes that were reflected in the model parameters. Second, the amount of motivation may not have been matched between the initial retreat and wait-list control groups, as the participants were aware of their group assignment prior to receiving meditation training. Although our wait-list design likely addressed several important design limitations of prior research on intensive meditation, future investigations should attempt to better account for various social, motivational, and environmental factors by using active control conditions or by comparing training periods of differing lengths.

Other limitations of this work come from the sparseness of cortical sampling (i.e., number of EEG sensors used and modeled). One future avenue of research could be to concurrently use high spatial resolution neuroimaging modalities (e.g., fMRI) for better modeling and understanding of neural data collected during meditation practice.

Another potential limitation concerns the quantification of IAF values. To calculate IAF values for each participant, we employed the widely used power-weighted (or center of gravity) method to determine mean alpha frequency across all channels (Klimesch, 1999). This power-weighted method provides an advantage over visual inspection based methods to find the peak alpha frequency: in cases where the EEG spectra have multiple peaks or are flat in the alpha range, power-weighted methods better reflect the central tendency of alpha power and are more representative of the underlying activity (Goljahani et al., 2012). However, to calculate power-weighted IAF, a predetermined interval of alpha frequencies is required. Defining such a priori intervals can lead to biased estimates, particularly when participants have a very high or low alpha peak. Thus, new automated methods, based on regression (Chiang et al., 2008) and channel selection (Goljahani et al., 2012) have been recently proposed. Future work

is thus required to carefully examine how the calculation of IAF using novel methods may influence the assessment of IAF values in long-term meditators.

Lastly, it is important to note that the modeling approach presented here, although widely accepted in the extant literature related to EEG-based computational models, is still very approximate in nature and is based on a number of assumptions. These assumptions are required to generate models that are computationally practical and tractable. We argue that such modeling approaches, while not mechanistically accurate, may still enable progress in understanding complex brain phenomenon. By simulating a complex phenomena (or associated neurophysiological correlates) based on an initial formulation, the goal of such approaches is to generate novel hypotheses that may motivate future research studies and data collection, and in turn refine the model and its underlying assumptions. Such a process implements the classic cycle of theory development, testing, and revision to advance our understanding.

Conclusions and future work

We present the first computational model of neurophysiological changes during shamatha and related FA meditation, which advances our previous work investigating scalp-recorded EEG during meditation by examining the putative role of corticothalamic and intrathalamic interactions in observed longitudinal changes in cortical activity associated with intensive meditation training. Our computational approach offers several testable hypotheses that could motivate the incorporation of shamatha and FA meditation in novel treatment approaches. Specifically, the observed decrease in intrathalamic gain parameter following training serves to motivate further study of shamatha and FA meditation as a potential treatment approach for individuals with ADHD, whereas increased model stability after training motivates further analysis of the potential efficacy of shamatha and FA meditation practice as part of treatment strategies for neurological disorders (e.g., epilepsy). Finally, a similar modeling approach can be applied to EEG data obtained during performance of cognitive tasks so that changes in model parameters can be directly related to training-related changes in measureable task performance.

References

Aftanas, L.I., Golosheikin, S.A., 2001. Human anterior and frontal midline theta and lower alpha reflect emotionally positive state and internalized attention: high-resolution EEG investigation of meditation. Neurosci. Lett. 310, 57–60.

Aftanas, L.I., Golosheikin, S.A., 2002. Non-linear dynamic complexity of the human EEG during meditation. Neurosci. Lett. 330, 143–146.

Aftanas, L.I., Golosheikin, S.A., 2003. Changes in cortical activity in altered states of consciousness: the study of meditation by high-resolution EEG. Hum. Physiol. 29, 143–151.

Austin, J.H., 2013. Zen and the brain: mutually illuminating topics. Front. Psychol. 4, 784. http://dx.doi.org/10.3389/fpsyg.2013.00784.

Banquet, J.P., 1973. Spectral analysis of the EEG in meditation. Electroencephalogr. Clin. Neurophysiol. 35, 143–151.

Belouchrani, A., Abed-Meraim, K., Cardoso, J.F., Moulines, E., 1993. Second-order blind separation of temporally correlated sources. Presented at the Proc. Int. Conf. Digital Signal Processing, pp. 346–351.

Bollimunta, A., Mo, J., Schroeder, C.E., Ding, M., 2011. Neuronal mechanisms and attentional modulation of corticothalamic α oscillations. J. Neurosci. 31, 4935–4943. http://dx.doi.org/10.1523/JNEUROSCI.5580-10.2011.

Breakspear, M., Roberts, J.A., Terry, J.R., Rodrigues, S., Mahant, N., Robinson, P.A., 2006. A unifying explanation of primary generalized seizures through nonlinear brain modeling and bifurcation analysis. Cereb. Cortex 16, 1296.

Brefczynski-Lewis, J.A., Lutz, A., Schaefer, H.S., Levinson, D.B., Davidson, R.J., 2007. Neural correlates of attentional expertise in long-term meditation practitioners. Proc. Natl. Acad. Sci. 104, 11483.

Bressler, S.L., Menon, V., 2010. Large-scale brain networks in cognition: emerging methods and principles. Trends Cogn. Sci. 14, 277–290. http://dx.doi.org/10.1016/j.tics.2010.04.004.

Cahn, B.R., Polich, J., 2006. Meditation states and traits: EEG, ERP, and neuroimaging studies. Psychol. Bull. 132, 32.

Callaway, E.M., 1998. Local circuits in primary visual cortex of the macaque monkey. Annu. Rev. Neurosci. 21, 47–74. http://dx.doi.org/10.1146/annurev.neuro.21.1.47.

Chiang, A.K.I., Rennie, C.J., Robinson, P.A., Roberts, J.A., Rigozzi, M.K., Whitehouse, R.W., Hamilton, R.J., Gordon, E., 2008. Automated characterization of multiple alpha peaks in multi-site electroencephalograms. J. Neurosci. Methods 168, 396–411. http://dx.doi.org/10.1016/j.jneumeth.2007.11.001.

Ching, S., Cimenser, A., Purdon, P.L., Brown, E.N., Kopell, N.J., 2010. Thalamocortical model for a propofol-induced alpha-rhythm associated with loss of consciousness. Proc. Natl. Acad. Sci. 107, 22665–22670. http://dx.doi.org/10.1073/pnas.1017069108.

Coleman, T.F., Li, Y., 1993. An Interior Trust Region Approach for Nonlinear Minimization Subject to Bounds. SIAM Journal on Optimization.

Corbetta, M., Shulman, G.L., 2002. Control of goal-directed and stimulus-driven attention in the brain. Nat. Rev. Neurosci. 3, 201–215. http://dx.doi.org/10.1038/nrn755.

Crabtree, J.W., Killackey, H.P., 1989. The topographic organization and axis of projection within the visual sector of the rabbit's thalamic reticular nucleus. Eur. J. Neurosci. 1, 94–109.

Crick, F., 1984. Function of the thalamic reticular complex: the searchlight hypothesis. Proc. Natl. Acad. Sci. U. S. A. 81, 4586.

Csicsvari, J., Jamieson, B., Wise, K.D., Buzsaki, G., 2003. Mechanisms of gamma oscillations in the hippocampus of the behaving rat. Neuron 37, 311–322.

Desbordes, G., Negi, L.T., 2013. A new era for mind studies: training investigators in both scientific and contemplative methods of inquiry. Front. Hum. Neurosci 7, 741. http://dx.doi.org/10.3389/fnhum.2013.00741.

Dosenbach, N.U.F., Fair, D.A., Cohen, A.L., Schlaggar, B.L., Petersen, S.E., 2008. A dual-networks architecture of top-down control. Trends Cogn. Sci. 12, 99–105. http://dx.doi.org/10.1016/j.tics.2008.01.001.

Englehardt, W., Carl, G., Dierks, T., Maurer, K., 1991. Electroencephalographic mapping during isoflurane anesthesia for treatment of mental depression. J. Clin. Monit. 7, 23–29.

Fan, J., McCandliss, B.D., Fossella, J., Flombaum, J.I., Posner, M.I., 2005. The activation of attentional networks. NeuroImage 26, 471–479. http://dx.doi.org/10.1016/j.neuroimage.2005.02.004.

Fox, K.C.R., Nijeboer, S., Dixon, M.L., Floman, J.L., Ellamil, M., Rumak, S.P., Sedlmeier, P., Christoff, K., 2014. Is meditation associated with altered brain structure? A systematic review and meta-analysis of morphometric neuroimaging in meditation practitioners. Neurosci. Biobehav. Rev. http://dx.doi.org/10.1016/j.neubiorev.2014.03.016.

Freeman, W.J., 1972. Linear analysis of the dynamics of neural masses. Annu. Rev. Biophys. Bioeng. 1, 225–256.

Freeman, W.J., 1975. Mass Action in the Nervous System. Academic Press New York.

Freeman, W.J., 1987. Simulation of chaotic EEG patterns with a dynamic model of the olfactory system. Biol. Cybern. 56, 139–150.

Friedman, M., 1937. The use of ranks to avoid the assumption of normality implicit in the analysis of variance. J. Am. Stat. Assoc. 32, 675–701.

Goldman, R.I., Stern, J.M., Engel Jr., J., Cohen, M.S., 2002. Simultaneous EEG and fMRI of the alpha rhythm. NeuroReport 13, 2487.

Goljahani, A., D'Avanzo, C., Schiff, S., Amodio, P., Bisiacchi, P., Sparacino, G., 2012. A novel method for the determination of the EEG individual alpha frequency. NeuroImage 60, 774–786. http://dx.doi.org/10.1016/j.neuroimage.2011.12.001.

Guglietti, C.L., Daskalakis, Z.J., Radhu, N., Fitzgerald, P.B., Ritvo, P., 2012. Meditation-related increases in GABAB modulated cortical inhibition. Brain Stimul. 1–6. http://dx.doi.org/10.1016/j.brs.2012.08.005.

Halassa, M.M., Siegle, J.H., Ritt, J.T., Ting, J.T., Feng, G., Moore, C.I., 2011. Selective optical drive of thalamic reticular nucleus generates thalamic bursts and cortical spindles. Nat. Neurosci. 14, 1118–1120. http://dx.doi.org/10.1038/nn.2880.

Hasenkamp, W., Barsalou, L.W., 2012. Effects of meditation experience on functional connectivity of distributed brain networks. Front. Hum. Neurosci. 6, 38. http://dx.doi.org/10.3389/fnhum.2012.00038.

Hasenkamp, W., Wilson-Mendenhall, C.D., Duncan, E., Barsalou, L.W., 2012. Mind wandering and attention during focused meditation: a fine-grained temporal analysis of fluctuating cognitive states. NeuroImage 59, 750–760. http://dx.doi.org/10.1016/j.neuroimage.2011.07.008.

Hölzel, B.K., Carmody, J., Vangel, M., Congleton, C., Yerramsetti, S.M., Gard, T., Lazar, S.W., 2011. Mindfulness practice leads to increases in regional brain gray matter density. Psychiatry Res. 191, 36–43. http://dx.doi.org/10.1016/j.pscychresns.2010.08.006.

Huerta, P.T., Lisman, J.E., 1995. Bidirectional synaptic plasticity induced by a single burst during cholinergic theta oscillation in CA1 in vitro. Neuron 15, 1053–1063.

Isaksson, A., Wennberg, A., Zetterberg, L.H., 1981. Computer analysis of EEG signals with parametric models. Proc. IEEE 69, 451–461.

Jha, A.P., Krompinger, J., Baime, M.J., 2007. Mindfulness training modifies subsystems of attention. Cogn. Affect. Behav. Neurosci. 7, 109–119.

Jirsa, V.K., Sporns, O., Breakspear, M., Deco, G., McIntosh, A.R., 2010. Towards the virtual brain: network modeling of the intact and the damaged brain. Arch. Ital. Biol. 148, 189–205.

Jones, E.G., 2009. Synchrony in the interconnected circuitry of the thalamus and cerebral cortex. Ann. N. Y. Acad. Sci. 1157, 10–23. http://dx.doi.org/10.1111/j.1749-6632.2009.04534.x.

Jones, S.R., Pritchett, D.L., Stufflebeam, S.M., Hämäläinen, M., Moore, C.I., 2007. Neural correlates of tactile detection: a combined magnetoencephalography and biophysically based computational modeling study. 27, 10751–10764. http://dx.doi.org/10.1523/JNEUROSCI.0482-07.2007.

Jones, S.R., Pritchett, D.L., Sikora, M.A., Stufflebeam, S.M., Hämäläinen, M., Moore, C.I., 2009. Quantitative analysis and biophysically realistic neural modeling of the MEG Mu rhythm: rhythmogenesis and modulation of sensory-evoked responses. J. Neurophysiol. 102, 3554–3572. http://dx.doi.org/10.1152/jn.00535.2009.

Jones, S.R., Kerr, C.E., Wan, Q., Pritchett, D.L., Hämäläinen, M., Moore, C.I., 2010. Cued spatial attention drives functionally relevant modulation of the mu rhythm in primary somatosensory cortex. J. Neurosci. 30, 13760–13765. http://dx.doi.org/10.1523/JNEUROSCI.2969-10.2010.

Kasamatsu, A., Hirai, T., 1966. An electroencephalographic study on the Zen meditation (Zazen). Psychiatry Clin. Neurosci. 20, 315–336.

Kastner, S., Saalmann, Y.B., Schneider, K.A., 2012. Thalamic Control of Visual Attention. Oxford University Press http://dx.doi.org/10.1093/acprof:oso/9780195334364.003.0003.

Kayser, J., Tenke, C.E., 2006. Principal components analysis of Laplacian waveforms as a generic method for identifying ERP generator patterns: I. Evaluation with auditory oddball tasks. Clin. Neurophysiol. 117, 348–368.

Kerr, C.C., Rennie, C.J., Robinson, P.A., 2008. Physiology-based modeling of cortical auditory evoked potentials. Biol. Cybern. 98, 171–184.

Kerr, C.C., van Albada, S.J., Rennie, C.J., Robinson, P.A., 2010. Age trends in auditory oddball evoked potentials via component scoring and deconvolution. Clin. Neurophysiol. 121, 962–976.

Kerr, C.C., Rennie, C.J., Robinson, P.A., 2011. Model-based analysis and quantification of age trends in auditory evoked potentials. Clin. Neurophysiol. 122, 134–147.

Kerr, C.E., Sacchet, M.D., Lazar, S.W., Moore, C.I., Jones, S.R., 2013. Mindfulness starts with the body: somatosensory attention and top-down modulation of cortical alpha rhythms in mindfulness meditation. Front. Hum. Neurosci. 7, 12. http://dx.doi.org/10.3389/fnhum.2013.00012.

Klimesch, W., 1999. EEG alpha and theta oscillations reflect cognitive and memory performance: a review and analysis. Brain Res. Rev. 29, 169–195.

Lagerlund, T.D., Sharbrough, F.W., 1989. Computer simulation of the generation of the electroencephalogram. Electroencephalogr. Clin. Neurophysiol. 72, 31.

Lam, Y.-W., Sherman, S.M., 2010. Functional organization of the somatosensory cortical layer 6 feedback to the thalamus. Cereb. Cortex 20, 13–24. http://dx.doi.org/10.1093/cercor/bhp077.

Lam, Y.-W., Sherman, S.M., 2011. Functional organization of the thalamic input to the thalamic reticular nucleus. J. Neurosci. 31 (18), 6791–6799. http://dx.doi.org/10.1523/JNEUROSCI.3073-10.2011.

Langri, T.J., 2009. Is Meditation a Means of Knowing our Mental World? [WWW Document] (URL andrewmacnairarchitect.com/FRANK%20BOOK/1.doc accessed 7.15.14).

Larson, C.L., Davidson, R.J., Abercrombie, H.C., Ward, R.T., Schaefer, S.M., Jackson, D.C., Holden, J.E., Perlman, S.B., 1998. Relations between PET-derived measures of thalamic glucose metabolism and EEG alpha power. Psychophysiology 35, 162–169.

Le Van Quyen, M., Navarro, V., Martinerie, J., Baulac, M., Varela, F.J., 2003. Toward a neurodynamical understanding of ictogenesis. Epilepsia 44 (Suppl. 12), 30–43.

Liley, D., Wright, J.J., 1994. Intracortical connectivity of pyramidal and stellate cells: estimates of synaptic densities and coupling symmetry. Netw. Comput. Neural Syst. 5, 175–189.

Lopes da Silva, F.H., Hoeks, A., Smits, H., Zetterberg, L.H., 1974. Model of brain rhythmic activity. Biol. Cybern. 15, 27–37.

Lumer, E.D., Edelman, G.M., Tononi, G., 1997. Neural dynamics in a model of the thalamocortical system. I. Layers, loops and the emergence of fast synchronous rhythms. Cereb. Cortex 7, 207.

Lutz, A., Thompson, E., 2003. Neurophenomenology Integrating Subjective Experience and Brain Dynamics in the Neuroscience of Consciousness. J. Conscious. Stud.

Lutz, A., Slagter, H.A., Dunne, J.D., Davidson, R.J., 2008. Attention regulation and monitoring in meditation. Trends Cogn. Sci. 12, 163–169.

Lutz, A., Slagter, H.A., Rawlings, N.B., Francis, A.D., Greischar, L.L., Davidson, R.J., 2009. Mental training enhances attentional stability: neural and behavioral evidence. J. Neurosci. 29, 13418.

MacLean, K.A., Ferrer, E., Aichele, S.R., Bridwell, D.A., Zanesco, A.P., Jacobs, T.L., King, B.G., Rosenberg, E.L., Sahdra, B.K., Shaver, P.R., Wallace, B.A., Mangun, G.R., Saron, C.D., 2010. Intensive meditation training improves perceptual discrimination and sustained attention. Psychol. Sci. 21, 829–839. http://dx.doi.org/10.1177/0956797610371339.

Maris, E., Oostenveld, R., 2007. Nonparametric statistical testing of EEG-and MEG-data. J. Neurosci. Methods 164, 177–190.

Maris, E., Schoffelen, J.M., Fries, P., 2007. Nonparametric statistical testing of coherence differences. J. Neurosci. Methods 163, 161–175.

MATLAB, 2010. The MathWorks Inc. Natick, MA.

McAlonan, K., Cavanaugh, J., Wurtz, R.H., 2008. Guarding the gateway to cortex with attention in visual thalamus. Nature 456, 391–394. http://dx.doi.org/10.1038/nature07382.

Meeren, H.K.M., Pijn, J.P.M., Van Luijtelaar, E.L.J.M., Coenen, A.M.L., Lopes da Silva, F.H., 2002. Cortical focus drives widespread corticothalamic networks during spontaneous absence seizures in rats. J. Neurosci. 22, 1480–1495.

Menon, V., 2011. Large-scale brain networks and psychopathology: a unifying triple network model. Trends Cogn. Sci. 15, 483–506. http://dx.doi.org/10.1016/j.tics.2011.08.003.

Mirowski, P., Madhavan, D., Lecun, Y., Kuzniecky, R., 2009. Classification of patterns of EEG synchronization for seizure prediction. Clin. Neurophysiol. 120, 1927–1940. http://dx.doi.org/10.1016/j.clinph.2009.09.002.

Mitchell, J.T., McIntyre, E.M., English, J.S., Dennis, M.F., Beckham, J.C., Kollins, S.H., 2013. A pilot trial of mindfulness meditation training for ADHD in adulthood: impact on core symptoms, executive functioning, and emotion dysregulation. J. Atten. Disord. http://dx.doi.org/10.1177/1087054713513328.

Mitra, P.P., Pesaran, B., 1999. Analysis of dynamic brain imaging data. Biophys. J. 76, 691–708.

Moore, A., Gruber, T., Derose, J., Malinowski, P., 2012. Regular, brief mindfulness meditation practice improves electrophysiological markers of attentional control. Front. Hum. Neurosci. 6, 18. http://dx.doi.org/10.3389/fnhum.2012.00018.

Newberg, A.B., Iversen, J., 2003. The neural basis of the complex mental task of meditation: neurotransmitter and neurochemical considerations. Med. Hypotheses 61, 282–291.

Nunez, P.L., 1974a. The brain wave equation: a model for the EEG. Math. Biosci. 21, 279–297.

Nunez, P.L., 1974b. Wavelike properties of the alpha rhythm. IEEE Trans. Biomed. Eng. 473–482.

Nunez, P.L., 1995. Neocortical Dynamics and Human EEG Rhythms. Oxford University Press, USA.

O'Connor, S.C., Robinson, P.A., 2004. Spatially uniform and nonuniform analyses of electroencephalographic dynamics, with application to the topography of the alpha rhythm. Phys. Rev. E 70, 11911.

Oostenveld, R., Fries, P., Maris, E., Schoffelen, J.M., 2011. FieldTrip: open source software for advanced analysis of MEG, EEG, and invasive electrophysiological data. Comput. Intell. Neurosci. 2011, 1.

Perrin, F., Pernier, J., Bertrand, O., Echallier, J.F., 1989. Spherical splines for scalp potential and current density mapping. Electroencephalogr. Clin. Neurophysiol. 72, 184–187.

Pizzagalli, D.A., 2007. Electroencephalography and high-density electrophysiological source localization. Handb. Psychophysiol. 3, 56–84.

Posner, M.I., Petersen, S.E., 1990. The attention system of the human brain. Ann. Rev. Neurosci 13 (1), 25–42.

Reimann, M.W., Anastassiou, C.A., Perin, R., Hill, S.L., Markram, H., Koch, C., 2013. A biophysically detailed model of neocortical local field potentials predicts the critical role of active membrane currents. Neuron 79, 375–390. http://dx.doi.org/10.1016/j.neuron.2013.05.023.

Rennie, C.J., Robinson, P.A., Wright, J.J., 1999. Effects of local feedback on dispersion of electrical waves in the cerebral cortex. Phys. Rev. E 59, 3320–3329.

Rennie, C.J., Robinson, P.A., Wright, J.J., 2002. Unified neurophysical model of EEG spectra and evoked potentials. Biol. Cybern. 86, 457–471.

Robinson, P.A., Rennie, C.J., Wright, J.J., 1997. Propagation and stability of waves of electrical activity in the cerebral cortex. Phys. Rev. E 56, 826–840.

Robinson, P.A., Rennie, C.J., Wright, J.J., Bourke, P.D., 1998. Steady states and global dynamics of electrical activity in the cerebral cortex. Phys. Rev. E 58, 3557–3571.

Robinson, P.A., Loxley, P.N., O'Connor, S.C., Rennie, C.J., 2001a. Modal analysis of corticothalamic dynamics, electroencephalographic spectra, and evoked potentials. Phys. Rev. E Stat. Nonlinear Soft Matter Phys. 63, 041909.

Robinson, P.A., Rennie, C.J., Wright, J.J., Bahramali, H., Gordon, E., Rowe, D.L., 2001b. Prediction of electroencephalographic spectra from neurophysiology. Phys. Rev. E 63, 21903.

Robinson, P.A., Rennie, C.J., Rowe, D.L., 2002. Dynamics of large-scale brain activity in normal arousal states and epileptic seizures. Phys. Rev. E 65, 41924.

Robinson, P.A., Rennie, C.J., Rowe, D.L., O'Connor, S.C., Wright, J.J., Gordon, E., Whitehouse, R.W., 2003a. Neurophysical modeling of brain dynamics. Neuropsychopharmacology 28, 74.

Robinson, P.A., Whitehouse, R.W., Rennie, C.J., 2003b. Nonuniform corticothalamic continuum model of electroencephalographic spectra with application to split-alpha peaks. Phys. Rev. E Stat. Nonlinear Soft Matter Phys. 68, 021922.

Rowe, D.L., Robinson, P.A., Rennie, C.J., 2004a. Estimation of neurophysiological parameters from the waking EEG using a biophysical model of brain dynamics. J. Theor. Biol. 231, 413–433.

Rowe, D.L., Robinson, P.A., Rennie, C.J., Harris, A.W., Felmingham, K.L., Lazzaro, I.L., Gordon, E., 2004b. Neurophysiologically-based mean-field modelling of tonic cortical activity in post-traumatic stress disorder (PTSD), schizophrenia, first episode schizophrenia and attention deficit hyperactivity disorder (ADHD). J. Integr. Neurosci. 3, 453.

Rowe, D.L., Robinson, P.A., Gordon, E., 2005. Stimulant drug action in attention deficit hyperactivity disorder (ADHD): inference of neurophysiological mechanisms via quantitative modelling. Clin. Neurophysiol. 116, 324–335.

Saggar, M., 2011. Computational Analysis of Meditation. Retrieved from University of Texas Digital Repository: Electronic Theses and Dissertations (Austin, TX).

Saggar, M., King, B.G., Zanesco, A.P., MacLean, K.A., Aichele, S.R., Jacobs, T.L., Bridwell, D.A., Shaver, P.R., Rosenberg, E.L., Sahdra, B.K., Ferrer, E., Tang, A.C., Mangun, G.R., Wallace, B.A., Miikkulainen, R., Saron, C.D., 2012. Intensive training induces longitudinal

changes in meditation state-related EEG oscillatory activity. Front. Hum. Neurosci. 6, 256. http://dx.doi.org/10.3389/fnhum.2012.00256.

Sahdra, B.K., MacLean, K.A., Ferrer, E., Shaver, P.R., Rosenberg, E.L., Jacobs, T.L., Zanesco, A.P., King, B.G., Aichele, S.R., Bridwell, D.A., Mangun, G.R., Lavy, S., Wallace, B.A., Saron, C.D., 2011. Enhanced response inhibition during intensive meditation training predicts improvements in self-reported adaptive socioemotional functioning. Emotion 11, 299–312. http://dx.doi.org/10.1037/a0022764.

Schreckenberger, M., Lange-Asschenfeldt, C., Lange-Asschenfeld, C., Lochmann, M., Mann, K., Siessmeier, T., Buchholz, H.-G., Bartenstein, P., Gründer, G., 2004. The thalamus as the generator and modulator of EEG alpha rhythm: a combined PET/EEG study with lorazepam challenge in humans. NeuroImage 22, 637–644. http://dx.doi.org/10.1016/j.neuroimage.2004.01.047.

Sherman, S.M., Guillery, R.W., 2006. Exploring the Thalamus and Its Role in Cortical Function. MIT press Cambridge, MA.

Shwedyk, E., Balasubramanian, R., Scott, R.N., 1977. A nonstationary model for the electromyogram. IEEE Trans. Biomed. Eng. 417–424.

Slagter, H.A., Lutz, A., Greischar, L.L., Francis, A.D., Nieuwenhuis, S., Davis, J.M., Davidson, R.J., 2007. Mental training affects distribution of limited brain resources. PLoS Biol. 5 (e138).

Slagter, H.A., Davidson, R.J., Lutz, A., 2011. Mental training as a tool in the neuroscientific study of brain and cognitive plasticity. Front. Hum. Neurosci. 5.

Smith, S.M., Nichols, T.E., 2009. Threshold-free cluster enhancement: addressing problems of smoothing, threshold dependence and localisation in cluster inference. NeuroImage 44, 83–98. http://dx.doi.org/10.1016/j.neuroimage.2008.03.061.

Speckmann, E.J., Altrup, U., 1993. Generation of cortical field potentials. Basic Mechanisms of the EEGpp. 29–40.

Srinivasan, R., Winter, W.R., Ding, J., Nunez, P.L., 2007. EEG and MEG coherence: measures of functional connectivity at distinct spatial scales of neocortical dynamics. J. Neurosci. Methods 166, 41–52. http://dx.doi.org/10.1016/j.jneumeth.2007.06.026.

Steriade, M., 2005. Cellular Substrates of Brain Rhythms.

Steriade, M., McCormick, D.A., Sejnowski, T.J., 1993. Thalamocortical oscillations in the sleeping and aroused brain. Science 262, 679.

Tang, V., Michaelis, R., Kwan, P., 2014. Psychobehavioral therapy for epilepsy. Epilepsy Behav. 32, 147–155. http://dx.doi.org/10.1016/j.yebeh.2013.12.004.

Traub, R.D., Jefferys, J.G.R., Whittington, M.A., 1997. Simulation of gamma rhythms in networks of interneurons and pyramidal cells. J. Comput. Neurosci. 4, 141–150.

van Albada, S.J., Kerr, C.C., Chiang, A., Rennie, C.J., Robinson, P.A., 2010. Neurophysiological changes with age probed by inverse modeling of EEG spectra. Clin. Neurophysiol. 121, 21–38.

Van Boxtel, A., 2001. Optimal signal bandwidth for the recording of surface EMG activity of facial, jaw, oral, and neck muscles. Psychophysiology 38, 22–34.

van Vugt, M.K., Jha, A.P., 2011. Investigating the impact of mindfulness meditation training on working memory: a mathematical modeling approach. Cogn. Affect. Behav. Neurosci. 11, 344–353. http://dx.doi.org/10.3758/s13415-011-0048-8.

Wallace, R.K., 1970. Physiological effects of transcendental meditation. Science 167, 1751.

Wallace, B.A., 2005. Balancing The Mind: a Tibetan Buddhist Approach To Refining Attention. Snow Lion Publications.

Wallace, B.A., 2006. The attention revolution: unlocking the power of the focused mind. Wisdom Pubns.

Walsh, R., Shapiro, S.L., 2006. The meeting of meditative disciplines and Western psychology: a mutually enriching dialogue. Am. Psychol 61 (3), 227–239. http://dx.doi.org/10.1037/0003-066X.61.3.227.

Wilson, M., Bower, J.M., 1992. Cortical oscillations and temporal interactions in a computer simulation of piriform cortex. J. Neurophysiol. 67, 981.

Wilson, H.R., Cowan, J.D., 1972. Excitatory and inhibitory interactions in localized populations of model neurons. Biophys. J. 12, 1–24.

Wilson, H.R., Cowan, J.D., 1973. A mathematical theory of the functional dynamics of cortical and thalamic nervous tissue. Biol. Cybern. 13, 55–80.

Wright, J.J., Kydd, R.R., Sergejew, A.A., 1990. Autoregression models of EEG. Biol. Cybern. 62, 201–210.

Zhang, J.Z., et al., 1988. EEG findings during special psychical state (Qi Gong state) by means of compressed spectral array and topographic mapping. Comput. Biol. Med. 18, 455–463.

Zikopoulos, B., Barbas, H., 2006. Prefrontal projections to the thalamic reticular nucleus form a unique circuit for attentional mechanisms. J. Neurosci. 26, 7348–7361. http://dx.doi.org/10.1523/JNEUROSCI.5511-05.2006.

Zikopoulos, B., Barbas, H., 2007. Circuits for multisensory integration and attentional modulation through the prefrontal cortex and the thalamic reticular nucleus in primates. Rev. Neurosci. 18, 417.

Zylowska, L., Ackerman, D.L., Yang, M.H., Futrell, J.L., Horton, N.L., Hale, T.S., Pataki, C., Smalley, S.L., 2008. Mindfulness meditation training in adults and adolescents with ADHD: a feasibility study. J. Atten. Disord. 11, 737–746. http://dx.doi.org/10.1177/1087054707308502.

Zylowska, L., Smalley, S.L., Schwartz, J.M., 2009. Mindful awareness and ADHD. Clinical Handbook of Mindfulness. Springer.